Hybrid Ferromagnetic/Ferroelectric Materials

10

Sebastiaan van Dijken

Contents

Abstract

Studies of coupled magnetic and ferroelectric phases have significantly intensified in the last decade, motivated by fundamental questions about ferroic order coexistence and their potential for nanoelectronics. Hybrid ferromagnetic/ferroelectric materials in which magnetoelectric interactions arise from charge modulation, exchange coupling, or strain transfer at composite interfaces are particularly promising because they allow for electric-field control of magnetism at temperatures that are compatible with practical device

S. van Dijken (✉)
NanoSpin, Department of Applied Physics, Aalto University, School of Science, Aalto, Finland
e-mail: sebastiaan.van.dijken@aalto.fi

Y. Xu et al. (eds.), *Handbook of Spintronics*,
DOI 10.1007/978-94-007-6892-5_18

applications. In this chapter, recent developments in this field are reviewed, with emphasis on magnetoelectric coupling in thin-film heterostructures, ferromagnetic/ferroelectric domain interactions, and electronic transport in ferroelectric tunnel junctions.

List of Abbreviations

FMR	Ferromagnetic resonance
FTJ	Ferroelectric tunnel junction
ME	Magnetoelectric
MERAM	Magnetoelectric random access memory
MRAM	Magnetic random access memory
MTJ	Magnetic tunnel junction
PEEM	Photoemission electron microscopy
PFM	Piezoresponse force microscopy
SQUID	Superconducting quantum interference device
STT	Spin transfer torque
TER	Tunneling electroresistance
TMR	Tunneling magnetoresistance
VSM	Vibrating sample magnetometry
XANES	X-ray absorption near edge spectroscopy
XMCD	X-ray magnetic circular dichroism

Introduction

Ferromagnetic thin films exhibit a stable and switchable magnetization that memory devices and sensors use to store information and detect magnetic fields. Ferroelectric layers, on the other hand, allow for a variety of intriguing applications by virtue of their piezoelectric, dielectric, and polarization switching properties. While each of these material groups is utilized in many practical applications, research on hybrid structures that contain both ferroic order states is still in its infancy. Yet, the coexistence of ferromagnetism and ferroelectricity in so-called multiferroic materials promises to unveil new physical phenomena and provide additional functionalities to novel electronic devices. One particularly promising prospect of efficiently coupled multiphase systems is the ability to tailor magnetic properties in an applied electric field and to control ferro- and dielectric effects by the application of a magnetic field. The scientific significance of ferromagnetic/ferroelectric phase coexistence is illustrated by an intense revitalization of studies on magnetoelectric coupling in recent years. Efficient coupling at the interfaces of two intrinsically very different materials can result in behavior that is very unusual, if not unprecedented, in naturally occurring compounds. The exploration of these effects offers significant opportunities for innovations in spintronics. In this chapter, the main developments within the field of ferromagnetic/ferroelectric heterostructures are reviewed.

Multiferroic Materials

While ordered electronic states such as ferromagnetism and ferroelectricity have long been a centerpiece of solid-state and material physics due to their fundamental relevance in the understanding of phase control and related thermodynamic properties, studies on multiple ferroic order coexistence have been far more limited. The reasons for this are related to the mutual exclusivity of the conventional mechanisms that drive ferromagnetism and ferroelectricity [1] and the inability of early studies to establish strong magnetoelectric (ME) coupling effects [2]. Driven by advances in thin-film growth techniques and improved computational capabilities, studies on multiferroics, however, have greatly intensified during the last decade. This has led to the identification of new single-phase materials with different mechanisms for the stabilization of multiple- order coexistence. In one class of multiferroic materials, magnetism and ferroelectricity occur independently from each other. As a result, the ferroic ordering temperatures differ significantly, and ME coupling between both ordering states tends to be weak. Examples of multiferroic materials that belong to this class include $BiFeO_3$ and $YMnO_3$. In a second, more recently discovered class of single-phase multiferroic materials, the ferroelectric polarization is induced by a spiraling or collinear magnetic spin structure. Examples include $TbMnO_3$, $Ni_3V_2O_6$, $TbMn_2O_5$, and YMn_2O_5. Due to the direct link between magnetism and ferroelectricity in these materials, ME coupling can be strong, but the induced polarization is small. Reviews on the physics of single-phase multiferroic materials can be found in Refs. [3–9]. For spintronic applications, materials that combine robust ferromagnetic and ferroelectric polarizations at room temperature and strong ME coupling are required. These attributes are more readily obtained in hybrid material systems, in which ferromagnetic and ferroelectric compounds are artificially assembled. This chapter focuses on ferromagnetic/ferroelectric heterostructures with emphasis on electric-field control of magnetism and transport phenomena. Electric-field effects in ferromagnetic thin films with dielectric gate oxides, which are also under intense investigation (see e.g., Refs. [10–19]), are outside the scope of this review.

Ferromagnetic/Ferroelectric Heterostructures

In hybrid ferromagnetic/ferroelectric material systems, ME coupling originates from direct or indirect interactions between two dissimilar ferroic phases at the heterostructure interfaces. Each material constituent of artificially assembled hybrids can be independently optimized for high-temperature operation, which facilitates their integration into practical devices. Moreover, since a wide variety of ferromagnetic and ferroelectric materials are available, the nature and strength of ME interactions can be systematically altered and maximized. This has led to the engineering of large ME responses that exceed those of single-phase multiferroic materials by several orders of magnitude [20–22].

At a macroscopic level, electric-field control of magnetism is often characterized by the converse ME coupling coefficient (α), which is defined as the change in magnetization upon the application of an electric field, i.e.,

$$\alpha = \mu_0 \Delta M / \Delta E \quad (1)$$

In SI, the unit of the converse ME coupling coefficient is sm^{-1}. The change in magnetization (ΔM) can be the result of an electric-field induced modification of the saturation magnetization, the exchange interaction, or the magnetic anisotropy. Large converse ME coupling coefficients have been obtained for vertical nanopillar arrays and horizontal thin-film heterostructures. Nanopillar arrays are often prepared by self-assembly during simultaneous deposition of two immiscible magnetic and ferroelectric compounds. Prototypical examples include combinations of ferroelectric perovskites (e.g., $BaTiO_3$, $PbTiO_3$, and $BiFeO_3$) and magnetic spinels (e.g., $CoFe_2O_4$, $NiFe_2O_4$, $MgFe_2O_4$, and Fe_3O_4) [23–33]. Integration of such nanocomposites on silicon substrates has been demonstrated [34]. Besides self-assembly, ordered arrays of magnetic/ferroelectric nanostructures have also been patterned using lithographic techniques [35–37] and hierarchical templating by polymer films [38].

For spintronic applications, electric-field control of magnetism in thin-film heterostructures is appealing because the layered geometry closely mimics the architecture of most spintronic devices (e.g., magnetic spin valves, magnetic tunnel junctions, and magnetic field-effect structures). Hence, the integration of horizontal ferromagnetic/ferroelectric thin-film hybrids into functional spintronic structures is more viable than materials that couple via vertically aligned interfaces. In particular, electric-field induced magnetic switching, magnetic domain wall motion, and dynamic spin precession are topics of intense current interest. In the last decade, researchers have successfully addressed these magnetic functions using the spin-transfer torque (STT) effect. In this actuation scheme, a spin-polarized current is passed through a magnetic thin film or magnetic domain wall, which results in current-induced magnetic switching, continuous spin precession, or the motion of magnetic domain walls under appropriate experimental conditions. The STT phenomenon now forms the basis for magnetic random access memories (MRAMs), tunable microwave oscillators, and magnetic nanowire device concepts [39, 40]. Employing electric currents, however, is inevitably accompanied by energy dissipation, and in this context, electric-field induced magnetic effects without major current flow are desirable. In ferromagnetic/ferroelectric thin-film heterostructures, a bias voltage is applied across the ferroelectric layer to alter the magnetic properties of an adjacent ferromagnetic film via ME coupling. Since the leakage current through the insulating ferroelectric layer is small, electric-field control of magnetism has the advantage of low power consumption. In addition, the integration of ferromagnetic/ferroelectric hybrid structures in practical devices opens up routes toward the combined use of both ferroic order parameters. Proposals in this direction include novel magnetic memories in which the data is written electrically and read magnetically [41–44], four-state memory cells based on multiferroic tunnel junctions [45–49], and electric-field tunable microwave devices [50–52].

In ferromagnetic/ferroelectric thin-film heterostructures, three converse ME coupling mechanisms have been explored, namely, (1) electric-field induced charge modulation, (2) electric-field controlled exchange interactions, and (3) piezoelectric or ferroelastic strain transfer. All coupling mechanisms can result in a modification of the saturation magnetization, the exchange interaction, or the magnetic anisotropy. Since charge modulation and exchange bias are both interface effects, electric-field control of magnetism via these ME coupling mechanisms is limited to thin ferromagnetic films. Moreover, exchange bias and ferroelastic strain transfer can be used to attain strong ferromagnetic–ferroelectric domain correlations. The prospects of this phenomenon are discussed in the section "Ferromagnetic/Ferroelectric Domain Coupling."

ME Coupling Based on Charge Modulation

At ferromagnetic/ferroelectric interfaces, ME coupling effects may originate from pure electronic mechanisms. Ab initio calculations and experiments indicate that electric fields can actively modify the magnetic and electronic properties of a variety of magnetic materials, including metallic ferromagnets [53–69], oxides [70–91], and dilute magnetic semiconductors [92–101]. One of the effects is related to the screening of electric fields by the accumulation or depletion of charge carriers in magnetic films. In ferromagnetic metals, electric fields are screened effectively by a high density of spin-polarized carriers. As a result, the spin imbalance at the Fermi level changes in an ultrathin region near the film interface, which alters the magnetic moment or magnetic anisotropy. For freestanding Fe, Ni, and Co films, the strength of the interface ME coupling coefficient is of the order $\alpha = 1.6 - 3 \times 10^{-22}$s [58]. Much larger values have been obtained for metallic ferromagnetic films on ferroelectric films or substrates. This difference is related to the proportionality between the screening charge of the metal and the dielectric constant of the ferroelectric material (typically, $\epsilon_r = 100$–1,000). For ferromagnetic/ferroelectric heterostructures, another electric-field effect originates from electronic hybridization between 3D transition metal atoms at the interface. For example, first-principle calculations based on density functional theory indicate that the magnetic moment of Fe atoms at a $Fe/BaTiO_3$ interface changes by about 5 % due to a shift in the Fe–Ti bond length during ferroelectric polarization reversal [53]. Similar effects have been found for $Co_2MnSi/BaTiO_3$ [55], $Fe/PbTiO_3$ [56, 62, 66], $Fe_3O_4/BaTiO_3$ [57], and $Co/PbZr_xTi_{1-x}O_3$ [67]. Markedly larger ME coupling effects based on ionic displacements at a $Fe/BaTiO_3$ interface are reported by Radaelli and coworkers [68]. In this work, it is convincingly demonstrated that exchange coupling in the interfacial-oxidized Fe layer can reversibly switch between antiferromagnetic and ferromagnetic upon out-of-plane polarization reversal in the $BaTiO_3$ layer.

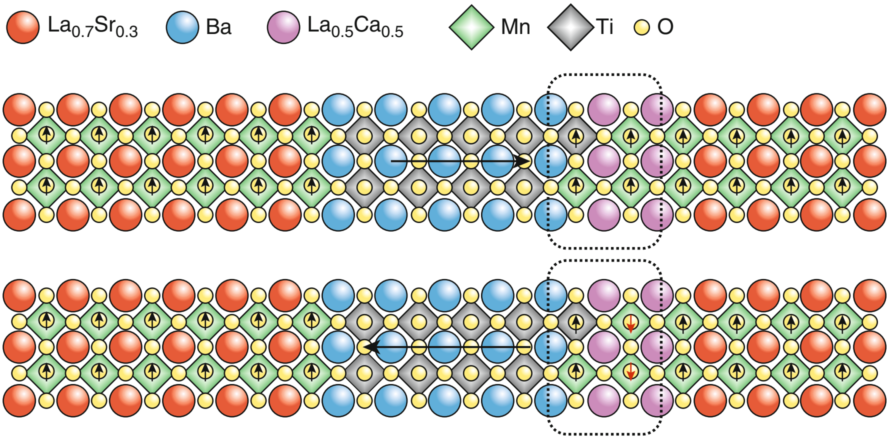

Fig. 1 Illustration of an electrically induced magnetic reconstruction at the $La_{0.5}Ca_{0.5}MnO_3$/$BaTiO_3$ interface (Reproduced from [85] with permission from Nature Publishing Group)

Electric-field effects based on charge modulation are particularly prominent in doped manganites due to strong lattice-spin-charge coupling. The accumulation or depletion of charge carriers near the interface of manganite films changes the hole doping concentration, a parameter that is normally controlled by substitution of La ions of the $LaMnO_3$ parent compound with alkaline earth ions. As a result, polarization reversal in an adjacent ferroelectric film can change the magnetic and electronic ground state of manganites when the material is positioned near one of its phase transitions. An example is shown in Fig. 1. First-principle calculations based on density functional theory indicate that the magnetic interface structure of $La_{0.5}A_{0.5}MnO_3$/$BaTiO_3$ (A = Sr, Ca, or Ba) is ferromagnetic when the polarization points toward the $La_{0.5}A_{0.5}MnO_3$ layer, while antiferromagnetically aligned Mn moments are obtained after polarization reversal [70, 71, 85]. According to the phase diagrams of $La_{1-x}A_xMnO_3$ [102], the ferromagnetic-to-antiferromagnetic conversion is accompanied by a metal-to-insulator transition. This effect can be used to induce large tunneling electroresistance in ferroelectric tunnel junctions (section "Ferroelectric Tunnel Junctions") [85, 86].

Electrostatic control of manganite thin films has also been observed in experiments [74–91]. For example, the temperature of magnetic phase transitions and the magnetoresistance of $La_{0.8}Sr_{0.2}MnO_3$ change upon polarization reversal in $PbZr_{0.2}Ti_{0.8}O_3$/$La_{0.8}Sr_{0.2}MnO_3$ field-effect structures [74, 75]. Magneto-optical Kerr effect measurements on similar ferromagnetic–ferroelectric bilayers confirm these observations [77]. The latter study also demonstrates hysteretic switching between two magnetization states in an applied electric field. X-ray absorption near edge spectroscopy (XANES) measurements indicate that this effect can be ascribed to an electrostatic modulation of the valence state of Mn ions [79]. A more detailed discussion on charge-mediated ME coupling effects is given in Ref. [22].

ME Coupling Based on Exchange Interactions

Many single-phase multiferroic materials are antiferromagnetic. Intrinsic coupling between the ferroelectric polarization and the antiferromagnetic spin lattice in such materials can therefore be utilized to electrically control the exchange bias interaction with an adjacent ferromagnetic film. In conventional ferromagnetic/antiferromagnetic heterostructures, exchange bias manifests itself most prominently by a shift of the magnetic hysteresis loop along the magnetic field axis [103, 104]. The addition of voltage control over this interlayer coupling phenomenon is of interest to spintronic applications, in particular if the magnetic changes are reversible and isothermal. Multiferroic materials that have been explored for studies on exchange bias include $YMnO_3$ [105], $LuMnO_3$ [106], and $BiFeO_3$ [107–117]. For NiFe/$YMnO_3$, the application of an electric field during cooling through the Néel temperature reduces the exchange bias field. The change in exchange bias has been attributed to a decrease of coupled antiferromagnetic/ferroelectric domain walls, which act as the main pinning centers for the magnetization of the NiFe film [105]. A similar effect, namely the unpinning of the NiFe film magnetization by electric-field induced motion of antiferromagnetic/ferroelectric domain walls, can explain full reversal of the exchange bias direction in NiFe/$LuMnO_3$ under the simultaneous application of magnetic and electric fields [106].

Room temperature exchange coupling effects have been obtained using $BiFeO_3$, which exhibits a Néel temperature of 643 K. The origin of exchange bias in metallic ferromagnetic films on $BiFeO_3$ depends on the type of ferroelectric domain walls in the $BiFeO_3$ crystal. If the domains are predominantly separated by 109° walls, the exchange bias field is inversely proportional to the ferroelectric domain size [108, 109]. This observation suggests that uncompensated spins in the domain walls are the main source of the exchange bias effect. For 71° walls, on the other hand, no shift in the hysteresis loop is measured [108, 113]. In this case, exchange interactions between the ferromagnetic film and $BiFeO_3$ result in an enhancement of the coercive field, which is explained by direct coupling to the canted moment of $BiFeO_3$ domains. The orientation of the canted moment in $BiFeO_3$ is strongly linked to the direction of ferroelectric polarization. As a consequence, rotation of the polarization produces a lateral modulation of exchange anisotropy in an adjacent ferromagnetic film. This effect can lead to ferroelectric/ferromagnetic domain correlations (section "Ferromagnetic/Ferroelectric Domain Coupling"), which form a strong basis for electric-field controlled magnetic switching in exchange-coupled systems [107, 110, 113, 116]. Ferroic domain correlation were first demonstrated in $Co_{0.9}Fe_{0.1}$/$BiFeO_3$ using a combination of piezoresponse force microscopy (PFM) and X-ray magnetic circular dichroism (XMCD) with photoemission electron microscopy (PEEM) [107]. In this work, the application of an in-plane electric field resulted in 71° polarization switching inside the $BiFeO_3$ layer, causing 90° rotations of the ferroelectric and magnetic domain walls. In a subsequent study by the same group, additional anisotropic magnetoresistance measurements were used to illustrate that opposite 71° ferroelectric switching events in neighboring domains can be used to reverse the net magnetization of a $Co_{0.9}Fe_{0.1}$ film via local 90° magnetization rotation inside the domains. An even higher degree of electric-field control was recently obtained by strain-engineering of double switching events in $BiFeO_3$, leading to full magnetization reversal in an adjacent ferromagnetic film [116]. Moreover, integration of such exchange-coupled bilayers in magnetic spin valves resulted in nearly equal electric-field and magnetic-field switchable magnetoresistance effects. A detailed review of electric-field control of magnetism using $BiFeO_3$-based heterostructures can be found elsewhere [117].

Finally, it is noted that electric-field control of exchange bias is not limited to multiferroic materials. In fact, some of the early studies focused on Cr_2O_3 [118, 119], which is a magnetoelectric antiferromagnet below 307 K. Reversible, isothermal, and global electric-field control of exchange bias has been obtained in Pd/Co multilayers deposited on the (0001) surface of a Cr_2O_3 single crystal [120].

ME Coupling Based on Strain Transfer

Electric-field control of magnetism using strain transfer from a piezoelectric or ferroelectric material is based on the generation of magnetoelastic anisotropy in an adjacent ferromagnetic film via inverse magnetostriction. Strain-induced changes of the atomic and electronic structure of ferromagnets can also alter other magnetic properties. This is most apparent for perovskite manganites such as $La_{1-x}Sr_xMnO_3$ [121–125], $La_{1-x}Ca_xMnO_3$ [122, 126], $La_{1-x}Sr_xCoO_3$ [127], and $La_{1-x}Ba_xMnO_3$ [128], for which electric-field induced changes of the Curie temperature and colossal magnetoresistance have been reported. Contrary to charge modulation and exchange bias interactions, ME coupling via strain transfer can be efficient up to relatively large magnetic film thickness (>100 nm) [125, 129]. The electric-field dependence of strain transfer from a piezoelectric material or a ferroelectric material with ferroelastic domains differs. The application of an electric field across a piezoelectric material produces a butterfly-shaped piezostrain curve (Fig. 2a). The magnetic response of an adjacent magnetic film tends to mimic this strain curve [122]. Consequently, the change of magnetization is approximately linear and mostly reversible in an applied electric field. Removing the electric field from the piezoelectric medium releases the piezostrain in the magnetic film, which restores the anisotropy of the piezoelectrically unstrained film. Thus, in the absence of other symmetry breaking anisotropy contributions, the electric-field induced magnetic state does not persist when the field is turned off. This volatility, however, can be circumvented by carefully designed anisotropy configurations.

The most used piezoelectric material is (1-x)$Pb(Mg_{1/3}Nb_{2/3})O_3$-x$PbTiO_3$ (PMN-PT), which is a well-known relaxor ferroelectric with excellent electromechanical and piezoelectric properties for compositions near the morphotropic phase boundary ($0.25 \leq \times \leq 0.35$) [130]. Piezostrain transfer from PMN-PT has been utilized to tune the magnetic properties of manganite [121, 122, 125, 126], ferrite [51, 131–135], and metallic ferromagnetic films [136–139] and to alter the electrical resistance of magnetic oxides [121, 123, 124, 126–128, 134]. Besides crystalline

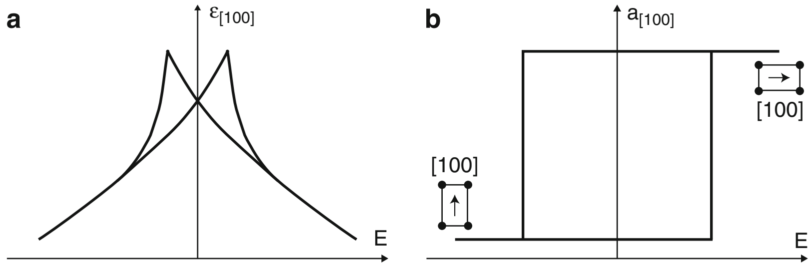

Fig. 2 Schematic illustration of the strain transfer curve of a piezoelectric material (**a**) and the variation of the in-plane lattice parameter during 90° in-plane polarization rotation in a tetragonal ferroelectric material (**b**). In the latter case, non-volatile switching between two ferroelastic domains can be used to alter the direction of uniaxial strain in an adjacent ferromagnetic film

substrates, commercial piezoelectric actuators have also been used to study voltage control of magnetic anisotropy [140–147].

Phenomenological models based on Landau free-energy thermodynamic theory [148–151] and phase field simulations [43, 44] have been used to analyze electric-field control of magnetism in ferromagnetic/piezoelectric heterostructures. By considering strain-induced variations of the magnetoelastic anisotropy energy, it is foreseen that the magnetic easy axis of $CoFe_2O_4$ and Ni can be reoriented from an in-plane to an out-of-plane direction [148, 149]. In-plane rotations of the magnetic easy axis at relatively small applied electric fields are also calculated for various other magnetic materials [150, 151]. Moreover, the temporal evolution of the magnetization configuration can be calculated by solving the Landau-Lifshitz-Gilbert equation in phase-field simulations. For nanometer-sized Ni elements on PMN-PT, switching times of the order of 1 ns have been predicted using this method [43, 44].

Potential applications of electric-field controlled ferromagnetic/piezoelectric heterostructures include electrically tunable microwave devices based on ferromagnetic resonance (FMR) and ME random access memory (MERAM). For example, giant electric-field tuning of the FMR frequency from 1.75 to 7.57 GHz in zero applied magnetic field for FeGaB films on (011) PZN-PT substrates (piezoelectric material similar to PMN-PT) has been demonstrated [50]. The wide-band tuning range in this experiment is ascribed to the large magnetostriction of FeGaB, which transforms the uniaxial piezostrain into a large in-plane magnetoelastic anisotropy. Similar results are obtained for Fe_3O_4 on PMN-PT and PZN-PT [51]. MERAM devices require nonvolatile magnetic switching in an applied electric field. Despite the intrinsic volatility of piezostrain, stable magnetic switching can be realized when a reversal to the original magnetic state is prevented by a competing magnetic anisotropy. The desired anisotropy configuration can be provided by a static magnetic field [142] or by other anisotropy contributions such as magnetocrystalline anisotropy [144] or exchange bias [152]. Other proposals for electric-field controlled deterministic magnetic switching involve the use of bistable piezostrain of partially poled piezoelectric layers [43, 44, 137], the hysteretic strain-voltage dependence of piezoelectric actuators [143], or dynamic strain effects in ferromagnetic films with perpendicular anisotropy [153]. Non-volatility can also be obtained by electric-field induced structural transitions between rhombohedral and orthorhombic phases in PMN-PT or PZN-PT crystals [135, 154]

Ferromagnetic/piezoelectric heterostructures have also been used to electrically alter the motion of magnetic domain walls [144, 155–158]. Electric-field control over the velocity of magnetic-field or current-driven magnetic domain walls is particularly efficient in the thermally activated dynamic creep regime. Here, the motion of magnetic domain walls depends sensitively on the disorder-induced pinning energy barrier and the depinning field [159], which can be tuned by transfer of piezoelectric strain and inverse magnetostriction. Local control over the pinning and depinning of magnetic domain walls has been realized by the patterning of side electrodes on hybrid $PbZr_{0.5}Ti_{0.5}O_3$/magnetic spin-valve structures [157]. Voltage-controlled magnetic domain wall gates and traps based on these concepts provide promising prospects for magnetic logic and memory technologies.

The characteristics of strain transfer from a ferroelectric material with ferroelastic domains are different from the mostly linear piezoelectric response. If the polarization reversal process involves the nucleation and growth of ferroelastic domains, i.e., domains that are separated by non-180° domain walls, the in-plane crystal lattice changes during ferroelectric switching (Fig. 2b). This hysteretic switching effect can be used to alter the magnetic properties of an adjacent ferromagnetic film in a nonvolatile way. The magnitude of transferrable strain depends on the ferroelectric material. For example, the tetragonal lattices of $PbTiO_3$ ($a = b = 3.905$ Å, $c = 4.156$ Å) [160] and $BaTiO_3$ ($a = b = 3.991$ Å, $c = 4.035$ Å) [161] provide a maximum uniaxial strain of 6.4 % and 1.1 % at room temperature. The strength of the induced magnetoelastic anisotropy depends on the efficiency of strain transfer and the magnetostrictive and elastic properties of the ferromagnetic material. Importantly, strain transfer from ferroelastic domains is not uniform but laterally modulated, which is schematically illustrated in Fig. 3. The local character of strain transfer allows for the imprinting of ferroelectric domains into ferromagnetic films and strong pinning of magnetic domain walls on top of ferroelectric domain boundaries. Before discussing these microscopic phenomena (section "Ferromagnetic/Ferroelectric Domain Coupling"), macroscopic measurements of strain-coupled ferromagnetic-ferroelectric heterostructures are reviewed first.

One popular approach in studies on elastic interactions between a ferroelectric material and a ferromagnetic film utilizes the structural phase transitions of $BaTiO_3$ substrates. The lattice structure of single-crystal $BaTiO_3$ changes as a function of decreasing temperature from cubic to tetragonal at 393 K, then from tetragonal to orthorhombic at 278 K, and finally from orthorhombic to rhombohedral at 183 K [162]. The concurrent changes of the $BaTiO_3$ domain pattern at these phase transitions alter the strain state of the ferromagnetic film, and via inverse magnetostriction, this can lead to local magnetic switching. In an early report by Lee and co-workers [163], the macroscopic response of $La_{0.67}Sr_{0.33}MnO_3$ films during cool down from 400 to 5 K was measured using SQUID magnetometry (Fig. 4).

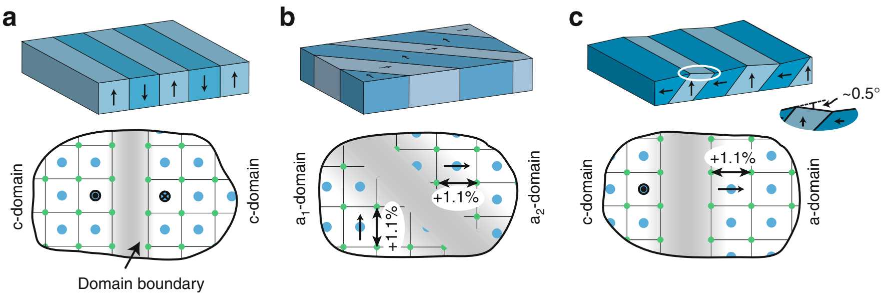

Fig. 3 Schematic illustration of domain patterns in tetragonal ferroelectric materials (e.g., $PbTiO_3$ and $BiTiO_3$ at room temperature) with a (001) crystal orientation. Polarization reversal between two out-of-plane states can be used for electrostatic control of magnetic properties (section "ME Coupling Based on Charge Modulation"), but the domain pattern in (**a**) does not modulate the lattice strain of an adjacent ferromagnetic film. Ferroelastic $a_1 - a_2$ (**b**) and $a - c$ (**c**) domain structures, on the other hand, can be used to attain ferromagnetic/ferroelectric domain correlations (section "Ferromagnetic/Ferroelectric Domain Coupling")

Fig. 4 Magnetization as a function of temperature for a 50 nm thick $La_{0.67}Sr_{0.33}MnO_3$ film on a $BaTiO_3$ (001) substrate. The *inset* shows magnetic hysteresis loops for temperatures below (T1) and above (T2) the orthorhombic-tetragonal structural phase transition of $BaTiO_3$ (Reproduced with permission from [163]. Copyright 2000, AIP Publishing LLC.)

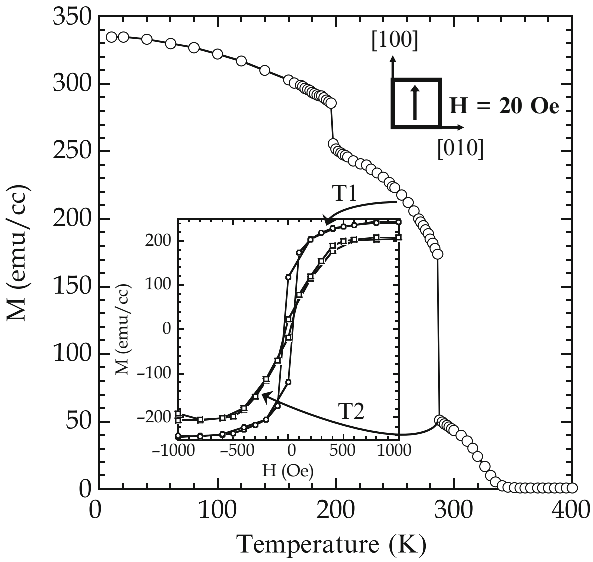

The abrupt changes in film magnetization at the phase transitions of $BaTiO_3$ are due to in-plane rotations of magnetic anisotropy caused by lattice distortions in the $BaTiO_3$ substrate. Similar magnetic effects are reported by other groups for a variety of materials. Besides $La_{1-x}Sr_xMnO_3$ [164], these include $La_{1-x}Ca_xMnO_3$ [165], Fe_3O_4 [166–168], Fe [169–174], Sr_2CrReO_6 [175], $CoFe_2O_4$ [176], SmCo [177], and exchange-biased Co/CoO bilayers [178]. Instant variations in sample magnetization at the phase transitions of $BaTiO_3$ are a common feature in these experiments, illustrating significant elastic coupling between the ferroelectric substrate and the ferromagnetic film. Most of the studies also report on coincident shifts in the coercive field and the remanent magnetization [166, 169, 172–175, 178]. These observations clearly indicate that abrupt changes in the ferroelastic domain pattern alter the strength and/or orientation of magnetic anisotropy. Macroscopic measurements, however, only reveal the average magnetic response. Due to the strong local character of strain transfer from ferroelastic domains, the change in magnetization varies from one domain to the other. Moreover, a variety of ferroelectric domain transformations can occur at the $BaTiO_3$ phase transitions, which complicates the interpretation of macroscopic data. Lahtinen et al. reported on temperature-induced local magnetic effects in CoFe films on $BaTiO_3$ substrates [179]. Optical polarization microscopy measurements in this study indicate local magnetization rotation by 90° during sample cooling and heating through the structural phase transitions of $BaTiO_3$.

Several experiments on electric-field control of magnetic films on top of $BaTiO_3$ substrates have been conducted [164, 169, 171, 173, 180–185]. Eerenstein and coworkers measured the magnetic response of $La_{0.67}Sr_{0.33}MnO_3$ films during the application of an out-of-plane electric field across the ferroelectric substrate using vibrating sample magnetometry (VSM) [164]. Sharp magnetic switching was obtained for electric fields in the range of 4–10 $kVcm^{-1}$ depending on sample temperature. Taniyama et al. reported on electric-field induced magnetic switching in rectangular Fe dots on $BaTiO_3$ [180]. In these experiments, a piezoresponse force microscope was used to apply local electric fields and the magnetic response was imaged using magnetic force microscopy. Electrical switching between single- and multidomain magnetic structures is demonstrated and ascribed to polarization reversal in the underlying ferroelectric substrate. In most experiments, the electric field is applied perpendicular to the $BaTiO_3$ substrate plane. Abrupt switching from in-plane to out-of-plane polarization alters the ferroelastic strain state in this configuration and via inverse magnetostriction the magnetoelastic anisotropy and coercive magnetic field are affected. ME coupling induced by the application of an in-plane electric field has been studied using suspended $BaTiO_3$/FeGa thin-film bilayer structures [186].

Besides anisotropy control, electric-field induced shifts of magnetic phase transitions can also be realized by strain transfer from ferroelastic domains. Reversible switching between antiferromagnetic and ferromagnetic order was recently demonstrated for FeRh films on $BaTiO_3$ substrates near a transition temperature of 350 K (Fig. 5) [187]. Tweaking of the magnetic phase in these experiments is ascribed to the growth of ferroelectric *c* domains at the expense of *a* domains in an out-of-plane electric field. Because of the giant change of magnetization during the electric-field induced ordering transition, the converse ME coupling coefficient is much larger than that of hybrid material systems based on anisotropy modulation.

In addition to $BaTiO_3$-based systems, electric-field control of magnetism via ferroelastic domain switching has also been demonstrated using PMN-PT and PZN-PT substrates [52, 188–191], providing large and nonvolatile magnetoelectric coupling effects. Moreover, strain-induced correlations between ferroelectric stripe domains in a $BiFeO_3$ layer and magnetic domains of a $La_{0.7}Sr_{0.3}MnO_3$ film have been imaged [192].

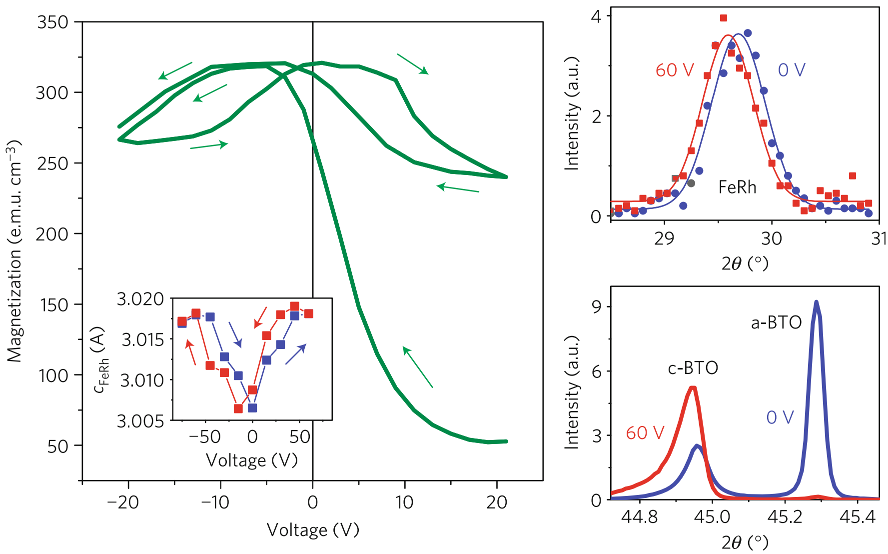

Fig. 5 Voltage dependence of magnetization in a FeRh/$BaTiO_3$ heterostructure at a temperature of 385 K. The change in magnetization is induced by ferroelastic domain switching in the $BaTiO_3$ substrate, as indicated by X-ray diffraction analysis (Reproduced from [187] with permission from Nature Publishing Group)

Ferromagnetic/Ferroelectric Domain Coupling

The local character of some ME coupling mechanisms and the direct link between the direction of ferroelectric polarization and the orientation of ME-induced magnetic anisotropy open up routes toward the design of ferromagnetic/ferroelectric heterostructures with correlated domain structures. In these hybrid material systems, rotation of the ferroelectric polarization alters the strength, orientation, and/or symmetry of the magnetic anisotropy in an adjacent ferromagnetic film. Moreover, the nearly instant change of magnetic anisotropy at ferroelectric domain boundaries creates a strong pinning potential for magnetic domain walls. Electric-field control of local magnetic switching, the writing and erasure of magnetic domain patterns, and the motion of magnetic domain walls can therefore be realized. In this section, the physics of domain pattern transfer in ferromagnetic/ferroelectric heterostructures is reviewed and the prospects for spintronic devices are discussed.

Domain Pattern Transfer

Domain pattern transfer from a ferroelectric material to a ferromagnetic film has been demonstrated in exchange-coupled CoFe/$BiFeO_3$ [107, 110, 113, 115, 116, 193] and strain-mediated ferromagnetic/$BaTiO_3$ [182–184, 194–199] and

$La_{0.7}Sr_{0.3}MnO_3/BiFeO_3$ [192] heterostructures. Exchange interactions between the canted magnetic moment of $BiFeO_3$ domains and an adjacent CoFe film can produce the required lateral modulation of magnetic anisotropy. The direct link between the direction of ferroelectric polarization and the orientation of the canted moment allows for electric-field control of magnetic domain patterns and local magnetization in this hybrid material system. Electric-field induced magnetic switching in $CoFe/BiFeO_3$ hybrids depends on the orientation of the $BiFeO_3$ film, the type of ferroelectric switching event (71° or 109° polarization rotation), and the direction of the applied electric field. The magnetic anisotropy strength of exchange-coupled heterostructures decreases with CoFe film thickness due to the interfacial character of the ME coupling mechanism. As a result, domain correlations vanish for relatively thin ferromagnetic films.

In strain-based systems, the ferroelastic domains of a ferroelectric material modulate the magnetoelastic anisotropy of an adjacent magnetic film via inverse magnetostriction. Full imprinting of ferroelastic domains into a magnetic film was first demonstrated for a CoFe film on top of a $BaTiO_3$ substrate with regular $a_1 - a_2$ domains (Fig. 6) [182]. The $a_1 - a_2$ domain pattern of tetragonal $BaTiO_3$ is characterized by 90° rotations of the ferroelectric polarization and uniaxial lattice elongation in the substrate plane (Fig. 3b). Domain correlations are obtained if the induced magnetoelastic anisotropy (K_{me}) dominates other magnetic energies, including the magnetocrystalline anisotropy (K_{mc}) and exchange and magnetostatic interactions between magnetic domains. Maximization of the anisotropy figure of merit K_{me}/K_{mc} thus provides a possible route towards the engineering of robust ferromagnetic/ferroelectric domain coupling. Ferroelastic $a - c$ stripe domains of $BaTiO_3$ can also be used to manipulate magnetic microstructures (Fig. 3c) [194, 195]. In this domain pattern, the ferroelectric polarization alternates between in-plane and out-of-plane. Because the out-of-plane c domains exhibit cubic in-plane structural symmetry, strain transfer from such domains induces a biaxial magnetic anisotropy in the adjacent ferromagnetic film. Imprinting of ferroelastic $a - c$ stripe patterns is therefore due to an abrupt change in anisotropy symmetry and strength at domain boundaries rather than a rotation of the uniaxial magnetoelastic anisotropy axis ($a_1 - a_2$ domains).

Strain-induced domain pattern transfer has been demonstrated for various ferromagnetic materials. Besides polycrystalline CoFe films [182–184], these include epitaxial Fe [194], epitaxial $CoFe_2O_4$ and $NiFe_2O_4$ [195], epitaxial manganites [192, 197], polycrystalline Ni [196] and NiFe [199], and amorphous CoFeB [198]. Magnetization reversal in these heterostructures is characterized by coherent magnetization rotation followed by abrupt magnetic switching within the domains (if K_{me} is sufficiently large). During this process, the magnetic domain walls are fully immobilized by strong pinning onto ferroelectric domain boundaries (Fig. 6). Since the magnetization of neighboring magnetic domains rotate in opposite directions, the total spin rotation within magnetic domain walls changes as a function of magnetic field strength [200]. Moreover, because of strong magnetic domain wall pinning, two distinctive magnetic microstructures can be initialized. Head-to-tail domain walls are formed when a magnetic field is applied perpendicular to the

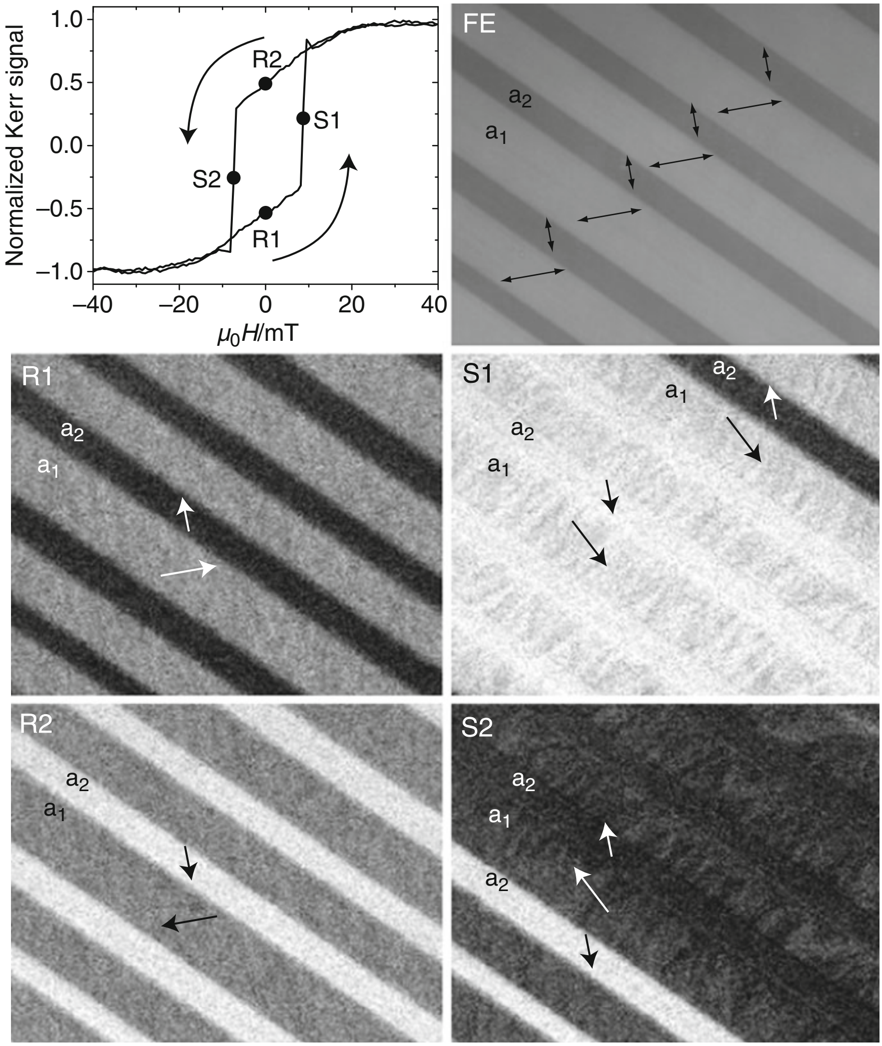

Fig. 6 Full domain pattern transfer from a ferroelectric $BaTiO_3$ substrate to a ferromagnetic CoFe thin film. Polarization microscopy and Kerr microscopy images show the domain structure of the ferroelectric (*FE*) and the domain pattern of the ferromagnet during several stages of the magnetization reversal process (*R1*, *S1*, *R2*, *S2*). The hysteresis curve represents an average magnetic response of many domains. The *arrows* in the images indicate the orientation of ferroelectric polarization (*FE*) and magnetization in the remanent states (*R1* and *R2*) and during abrupt magnetic switching (*S1* and *S2*) (Reproduced from [182] with permission from John Wiley and Sons)

stripe domains. In this case, the width of magnetic domain walls is mostly determined by the exchange stiffness and the strength of K_{me}. A magnetic field parallel to the stripe domains stabilizes alternating head-to-head and tail-to-tail domain walls. In this configuration, the width of the walls is mainly defined by magnetostatic interactions and magnetic anisotropy. Deterministic switching between magnetic walls with different width and energy can therefore be realized by in-plane rotation of the magnetic field [200]. This high degree of tunability could open the door to new magnetic devices wherein domain walls are utilized as functional and controllable elements.

Size Dependence of Domain Pattern Transfer

The physics of domain pattern transfer in hybrid ferromagnetic/ferroelectric materials is governed by a competition between the strength of the induced magnetic anisotropy and other relevant energies within the magnetic film. In particular, exchange and magnetostatic interactions oppose the formation of regular magnetic domains. For small ferroelectric domains, ferromagnetic coupling between neighboring domains exceeds the magnetic anisotropy and, hence, domain pattern transfer is no longer obtained. The cross-over from strong ferromagnetic/ferroelectric domain correlations to uniform film magnetization occurs when the width of the ferroelectric domains (Δ) becomes comparable to the width of the magnetic domain walls (δ) (Fig. 7) [201]. Two different scaling regimes are accessible. If the magnetic domains are separated by head-to-tail domain walls, the anisotropy and exchange energy determine the magnetic microstructure. In this case, the remanent spin rotation between neighboring domains diminishes when $\Delta \approx \delta \approx \pi\sqrt{A/2K_{me}}$, which is the width of 90° Néel walls when magnetostatic interactions are omitted [202]. Based on this analysis, a phase diagram for domain pattern transfer as a function of magnetic anisotropy can be constructed, as illustrated in Fig. 7c. For head-to-head and tail-to-tail magnetic domain walls, breakdown of domain pattern transfer is mainly determined by the anisotropy and magnetostatic energy of the system. Because magnetostatic coupling between domains extends over a longer distance than exchange interactions, the magnetization of neighboring domains are forced to align parallel at considerable larger domain width. In this case, domain pattern transfer breaks down when $\Delta \approx \delta \approx \pi \mu_0 M_s^2 t/8K_{me}$, which approximates half the width of 180° charged domain walls [203]. Thus contrary to uncharged walls, the critical length scale for domain patterns with magnetically charged walls increases linearly with ferromagnetic film thickness.

Electric-Field Control of Local Magnetic Switching and Magnetic Domain Patterns

The strong link between the direction of ferroelectric polarization and the orientation of magnetic anisotropy in hybrid materials with correlated domain structures enables

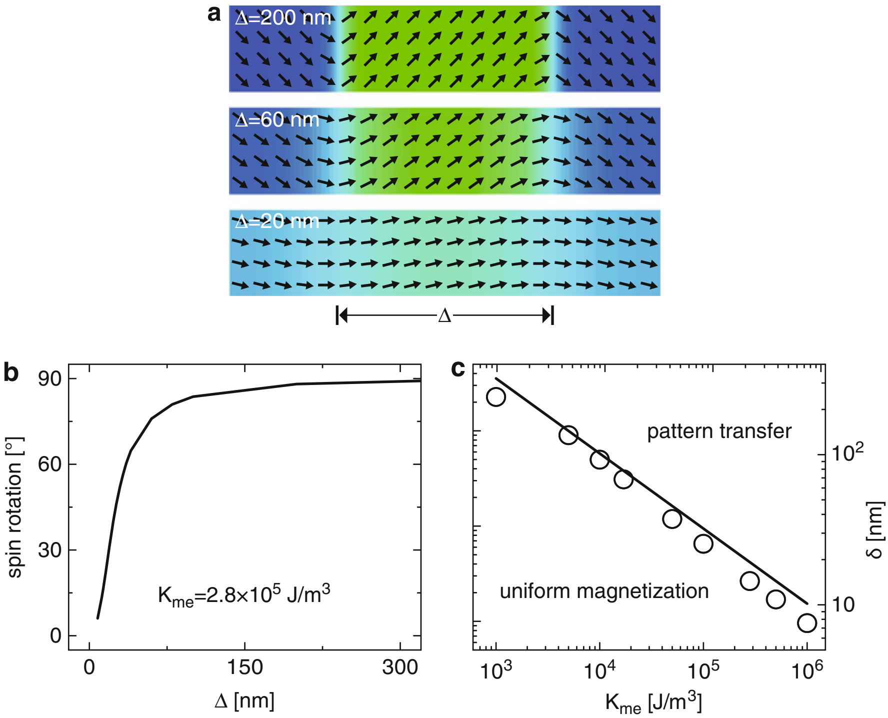

Fig. 7 (**a**) Micromagnetic simulations illustrating the breakdown of domain pattern transfer with decreasing ferroelectric domain width (Δ). (**b**) Dependence of domain wall spin rotation on Δ. (**c**) Phase diagram of domain pattern transfer as a function of magnetic anisotropy strength. The transition from a well-defined magnetic stripe pattern to uniform magnetization occurs when $\Delta \approx \delta$. The symbols and line indicate simulation data for δ and a calculation based on $\delta \approx \pi\sqrt{A/2K_{me}}$

electric-field control of local magnetic switching and magnetic domain patterns. Electric-field induced changes in ferroelectric domains are transferred to the ferromagnetic film if ME coupling at the interface is effective. In that case, concurrent rotations of the in-plane ferroelectric polarization (or its projection) and the magnetic anisotropy axis can trigger magnetic switching in zero magnetic field. In exchange-coupled CoFe/$BiFeO_3$ heterostructures, switching depends on the alignment between the ferroelectric polarization and the canted magnetic moment inside $BiFeO_3$ domains and interface exchange interactions with the magnetization of the CoFe film [48, 49, 107, 110, 113, 116]. For example, in the experiments of Ref. [113], the in-plane projection of ferroelectric polarization and easy anisotropy axis are collinear. Application of an in-plane electric field to this hybrid system results in 71° polarization switching between two <111> directions in $BiFeO_3$, which corresponds to a 90° rotation of the projected polarization in the (001) plane. Because of efficient ME coupling at the interface, the local magnetization of the CoFe film is forced to rotate by 90°. Full magnetization reversal in CoFe, i.e., switching by 180°, requires the engineering of more complicated double switching events in $BiFeO_3$, which was successfully demonstrated by Heron and coworkers [116].

Strain coupling to ferroelastic domains of a ferroelectric material offers another route towards non-volatile magnetic switching. Application of an out-of-plane electric field to a CoFe/$BaTiO_3$ heterostructure with fully correlated $a_1 - a_2$ domains (Fig. 6), for example, deterministically rotates the in-plane magnetization of the CoFe domains by 90° [182–184]. The regular magnetic stripe pattern is conserved during this switching event. However, when the ferroelectric polarization relaxes back into the plane of the $BaTiO_3$ substrate, the magnetic domain pattern disappears. The writing and erasure of regular magnetic stripes in zero magnetic field is reversible and it is fully explained by considering local strain transfer from ferroelastic $BaTiO_3$ domains to the CoFe film and modifications of magnetic anisotropy via inverse magnetostriction.

Electric-Field Driven Magnetic Domain Wall Motion

Domain coupling between a ferromagnetic film and a ferroelectric material also provides a platform for electric-field control of magnetic domain wall motion [184, 204, 205]. Abrupt changes in magnetic anisotropy at ferroelectric domain boundaries create a strong pinning potential for magnetic domain walls. This pinning effect fully immobilizes magnetic domain walls during magnetization reversal in an external magnetic field (section "Domain Pattern Transfer"). However, if a ferroelectric domain boundary is moved laterally by an applied electric field, the magnetic domain wall is forced to move along by a concurrent displacement of the pinning potential. An example of reversible electric-field driven magnetic domain wall motion is shown in Fig. 8. In this experiment, an epitaxial Fe film is elastically coupled to an $a - c$ domain structure of a $BaTiO_3$ substrate and an out-of-plane electric field is applied. If the electric field is aligned along the direction of ferroelectric polarization in the c domain (negative voltage pulse), the c domain grows at the expense of the neighboring a domain by lateral domain wall motion. A positive bias voltage, on the other hand, shrinks the c domain by moving the ferroelectric boundary in the opposite direction. Strong elastic pinning necessitates that the magnetic domain wall in the Fe film strictly follows the displacement of the ferroelectric domain boundary. Other configurations such as the motion of $a_1 - a_2$ magnetic domain walls driven by in-plane electric fields can also be considered, but this requires a network of planar electrodes and has not been explored yet. Initial studies on the dynamics of pinned magnetic/ferroelectric domain walls indicate several effects, including the emission of monochromatic spin waves, domain wall depinning, and oscillatory motion at high velocities [204, 205]. Since electric-field driven magnetic domain wall motion in hybrid heterostructures is only emerging, it is anticipated to gain scientific interest in the coming years.

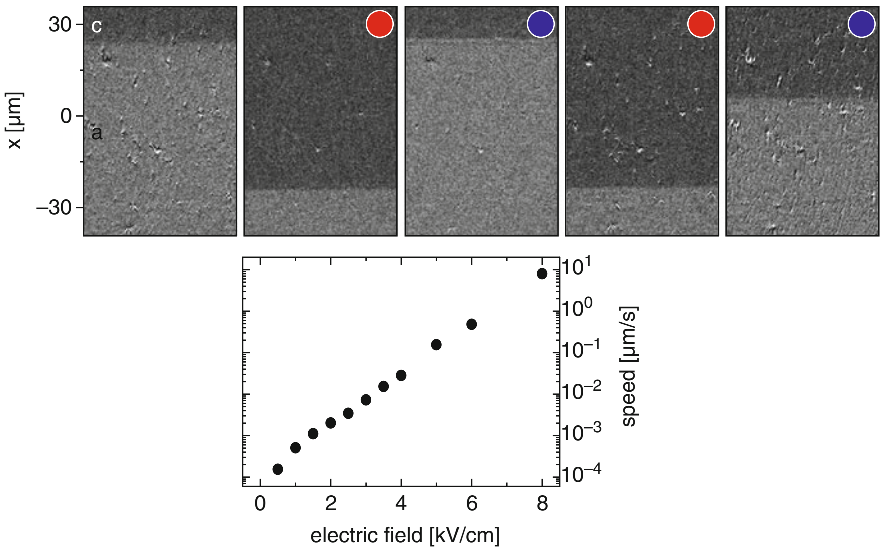

Fig. 8 Reversible electric-field driven magnetic domain wall motion in a 20 nm thick Fe film on a $BaTiO_3$ substrate. The Kerr microscopy images show the domain wall position after application of positive (*blue dots*) and negative (*red dots*) voltage pulses across the $BaTiO_3$ substrate. The dependence of magnetic domain wall velocity on electric field strength is shown in the graph. All measurements were conducted in zero magnetic field (Reproduced from Franke et al., Reversible Electric-Field-Driven Magnetic Domain-Wall Motion [204]. doi:http://dx.doi.org/10.1103/PhysRevX.5.011010)

Ferroelectric Tunnel Junctions

Ferromagnetic/ferroelectric thin-film heterostructures are often used in ferroelectric tunnel junctions (FTJs). In the most general form, an FTJ consists of a thin ferroelectric tunnel barrier and two conducting electrodes. Switching of the out-of-plane ferroelectric polarization by a bias voltage changes the junction resistance, an effect known as tunneling electroresistance (TER). Several mechanisms can contribute to TER [206], including (a) an electrostatic effect due to electric field-induced polarization reversal in the ferroelectric barrier, (b) an interface effect resulting from ionic displacements within the interface layers of the electrodes, and (c) a piezoelectric effect that alters the effective width of the tunnel barrier. In most experimental realizations [48, 49, 64, 85, 86, 207–219], the FTJ consists of a $BaTiO_3$, $PbTiO_3$, or $PbZr_xTi_{1-x}O_3$ barrier grown on top of a $La_{1-x}Sr_xMnO_3$ bottom electrode ($SrRuO_3$ in Ref. [209–211]). The top contact is either a metal or another conducting oxide. Epitaxial barrier/$La_{1-x}Sr_xMnO_3$ combinations are used to stabilize the out-of-plane ferroelectric polarization of the tunnel barrier via compressive in-plane lattice strain. Using piezo-response force microscopy (PFM), Garcia et al. have shown that the ferroelectric polarization of ultrathin $BaTiO_3$ films on $La_{0.67}Sr_{0.33}MnO_3$ can be retained down to a film thickness

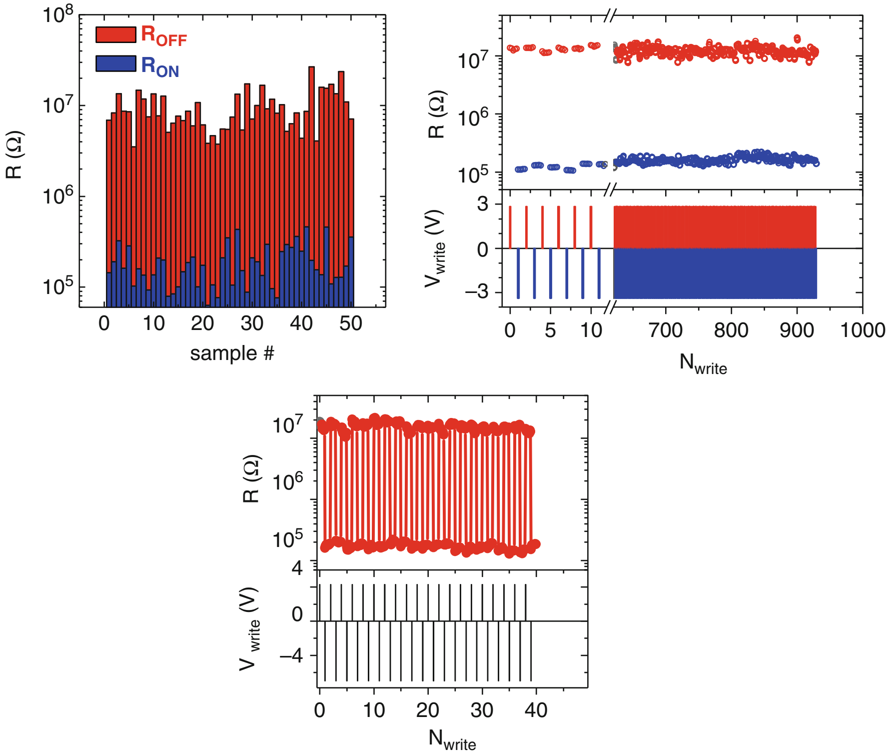

Fig. 9 OFF and ON resistance states of nanoscale FTJs with a 10 nm Co/2 nm $BaTiO_3$/30 nm $La_{0.67}Sr_{0.33}MnO_3$ structure (Reproduced from [214] with permission from Nature Publishing Group)

of only 1 nm [207]. Junctions with single-phase multiferroic tunnel barriers have also been studied [45, 220–224].

In FTJs with a metallic top electrode, a TER effect is caused by incomplete screening of polarization charges at the barrier/electrode interfaces, which for inherently different electrode materials leads to an asymmetrical deformation of the barrier potential [225, 226]. In this case, reversal of the barrier polarization produces two distinctive barrier heights and consequently two different tunnel barrier resistances. This scenario is supported by an exponential increase of the TER effect with tunnel barrier thickness [207]. The TER of FTJs with an asymmetrical barrier can be considerably larger than the tunneling magnetoresistance (TMR) of conventional magnetic tunnel junctions (MTJs). The maximum TMR effect at room temperature is about 600 % for MgO-based MTJs with CoFeB electrodes [227], which corresponds to an OFF/ON ratio of 7. However, for FTJs with a $La_{0.67}Sr_{0.33}MnO_3$ bottom electrode, a $BaTiO_3$ tunnel barrier, and a Co top electrode, OFF/ON ratios as high as 100 have been obtained (Fig. 9) [214]. Moreover, ferroelectric switching between the two resistance states only requires a

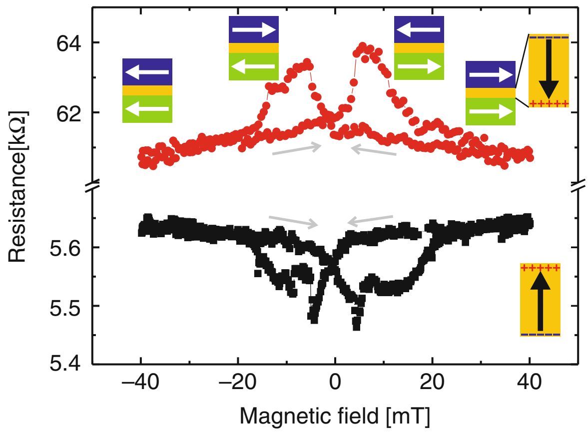

Fig. 10 Electric-field induced reversal of TMR in a Co/$PbZr_{0.2}Ti_{0.8}O_3$/$La_{0.7}Sr_{0.3}MnO_3$ tunnel junction. Negative TMR is obtained when the ferroelectric polarization of the $PbZr_{0.2}Ti_{0.8}O_3$ tunnel barrier points towards the Co top electrode. Polarization reversal by a voltage pulse of +3 V changes the sign of the TMR effect (Reproduced from [214] with permission from Nature Publishing Group)

current density of about 10^4 Acm^{-2}, which is considerably smaller than the critical current density for spin-transfer torque writing in MTJs ($\approx 10^6$ Acm^{-2}). The large, stable, and reproducible TER effect underpins the potential of FTJs for data storage applications. Further advances in strain engineering and careful control of electrical boundary conditions are anticipated to further enhance the performance of FTJs beyond the current state-of-the-art.

The resistance of FTJs with two ferromagnetic electrodes also changes in an applied magnetic field. The magnitude or even sign of the TMR effect can change upon polarization reversal in the ferroelectric tunnel barrier [48, 49, 64, 228]. Experiments on Co/$PbZr_{0.2}Ti_{0.8}O_3$/$La_{0.7}Sr_{0.3}MnO_3$ indicate that the TMR response is negative when the polarization points toward the Co electrode, while positive TMR is measured after ferroelectric switching into the opposite direction (Fig. 10) [49]. The polarization-induced modification of the TMR effect can be attributed to an anti-aligned induced magnetic moment on the Ti ions at the Co interface or a spin-dependent electrostatic screening effect in the interfacial layers of $La_{0.7}Sr_{0.3}MnO_3$. Support for the first scenario has been obtained by X-ray resonant magnetic scattering experiments [228] and first-principles calculations [53, 55–57, 66]. It has been argued that a combination of deterministic TER and TMR effects in single tunnel junctions could be utilized for the design of four-state memory cells.

Besides metallic electrode/ferroelectric barrier/$La_{1-x}Sr_xMnO_3$ junctions, large TER effects have also been obtained in all-oxide FTJs. Yin et al. reported on a TER response of 5,000 % at 40 K in 30 nm $La_{0.7}Sr_{0.3}MnO_3$/0.4–2 nm $La_{0.5}Ca_{0.5}MnO_3$/3 nm $BaTiO_3$/50 nm $La_{0.7}Sr_{0.3}MnO_3$ [85]. The TER of this heterostructure originates from electrostatic charge modulation in the $La_{0.5}Ca_{0.5}MnO_3$ insertion layer. When the barrier polarization points toward $La_{0.5}Ca_{0.5}MnO_3$, the layer is ferromagnetic and metallic. Polarization reversal away from the $La_{0.5}Ca_{0.5}MnO_3$/$BaTiO_3$ interface results in local hole accumulation, which changes the phase of the manganite layer to antiferromagnetic and insulating. As the junction resistance depends exponentially on the effective barrier width, large effects are readily obtained when only a few atomic layers of $La_{0.5}Ca_{0.5}MnO_3$ are affected by polarization reversal. As discussed in section "ME Coupling Based on Charge Modulation," the ability to induce phase transitions in thin-film manganites with appropriate doping concentration is supported by calculations and other experiments.

Finally, it is noted that giant TER effects have also been obtained for junctions wherein a ferroelectric $BaTiO_3$ tunnel barrier is directly grown onto a semiconducting Nb-doped $SrTiO_3$ substrate [229]. In this case, the effective tunnel barrier width is drastically altered by polarization-controlled accumulation or depletion of majority charge carriers at the semiconductor interface. The reported OFF/ON resistance ratio of FTJs with a semiconductor electrode is about 10^4 at room temperature.

Based on the recent progress in FTJs, their application in future memory and logic devices seems credible. Key advantages of FTJs include giant electroresistance, nondestructive readout, and low power usage. Moreover, the physical mechanisms behind TER are scalable to the nanometer range. Before commercialization, however, a number of scientific challenges related to the fatigue and retention characteristics of ultrathin ferroelectric films need to be solved.

Summary

Theoretical and experimental investigations of ferromagnetic/ferroelectric heterostructures have drastically intensified in the last decade. The potential use of these hybrid materials as electric-field controllable elements in spintronic devices offers several benefits including low power consumption and giant electroresistance. Two research directions can be distinguished based on the alignment of ferroelectric polarization. In structures with in-plane polarization, correlations between ferromagnetic and ferroelectric domains can be attained via local ME coupling. This enables electric-field control of nonvolatile magnetic switching, writing of magnetic domain patterns, and reversible magnetic domain wall motion. For practical applications of these effects, open questions related to the dynamics of ferromagnetic/ferroelectric domain coupling need to be answered. Ferroelectric materials with out-of-plane polarization can be used to modulate charge carriers in the interfacial layers of an adjacent ferromagnetic film. Ferroelectric tunnel junctions are based on this concept. Recent progress on tunneling electroresistance at room temperature offers promising prospects for innovations in nanoelectronics.

Acknowledgments The author thanks Kévin Franke and Tuomas Lahtinen for their contribution to the figures and John Burton, Evgeny Tsymbal, Chang-Beom Eom, Marin Alexe, Vincent Garcia, and Manuel Bibes for providing data. Financial support from the European Research Council (ERC-2012-StG 307502-E-CONTROL) is gratefully acknowledged.

References

1. Hill NA (2000) Why are there so few magnetic ferroelectrics? J Phys Chem B 104:6694
2. Fiebig M (2005) Revival of the magnetoelectric effect. J Phys D Appl Phys 38:123
3. Prellier W, Singh MP, Murugavel P (2005) The single-phase multiferroic oxides: from bulk to thin film. J Phys Condens Matter 17:803
4. Eerenstein W, Mathur ND, Scott JF (2006) Multiferroic and magnetoelectric materials. Nature 442:759
5. Ramesh R, Spaldin NA (2007) Multiferroics: progress and prospects in thin films. Nat Mater 6:21
6. Kimura T (2007) Spiral magnets as magnetoelectrics. Ann Rev Mater Sci 37:387
7. Catalan G, Scott JF (2009) Physics and applications of bismuth ferrite. Adv Mater 21:2463
8. Wang KF, Liu J-M, Ren ZF (2009) Multiferroicity: the coupling between magnetic and polarization orders. Adv Physiol Educ 58:321
9. Khomskii D (2009) Classifying multiferroics: mechanisms and effects. Physics 2:20
10. Maruyama T, Shiota Y, Nozaki T, Ohta K, Toda N, Mizuguchi M, Tulapurkar AA, Shinjo T, Shiraishi M, Mizukami S, Ando Y, Suzuki Y (2009) Large voltage-induced magnetic anisotropy change in a few atomic layers of iron. Nat Nanotechnol 4:158
11. Chiba D, Fukami S, Shimamura K, Ishiwata N, Kobayashi K, Ono T (2011) Electrical control of the ferromagnetic phase transition in cobalt at room temperature. Nat Mater 10:853
12. Shiota Y, Nozaki T, Bonell F, Murakami S, Shinjo T, Suzuki Y (2012) Induction of coherent magnetization switching in a few atomic layers of FeCo using voltage pulses. Nat Mater 11:39
13. Wang W-G, Li M, Hageman S, Chien CL (2012) Electric-field-assisted switching in magnetic tunnel junctions. Nat Mater 11:64
14. Nozaki T, Shiota Y, Miwa S, Murakami S, Bonell F, Ishibashi S, Kubota H, Yakushiji K, Saruya T, Fukushima A, Yuasa S, Shinjo T, Suzuki Y (2012) Electric-field-induced ferromagnetic resonance excitation in an ultrathin ferromagnetic metal layer. Nat Phys 8:492
15. Bauer U, Emori S, Beach GSD (2012) Electric field control of domain wall propagation in Pt/Co/GdOx films. Appl Phys Lett 100:192408
16. Schellekens AJ, van den Brink A, Franken JH, Swagten HJM, Koopmans B (2012) Electric-field control of domain wall motion in perpendicularly magnetized materials. Nat Commun 3:847
17. Chiba D, Kawaguchi M, Fukami S, Ishiwata N, Shimamura K, Kobayashi K, Ono T (2012) Electric-field control of magnetic domain-wall velocity in ultrathin cobalt with perpendicular magnetization. Nat Commun 3:888
18. Bauer U, Emori S, Beach GSD (2013) Voltage-controlled domain wall traps in ferromagnetic nanowires. Nat Nanotechnol 8:411
19. Bauer U, Yao L, Tan AJ, Agrawal P, Emori S, Tuller HL, van Dijken S, Beach GSD (2015) Magneto-ionic control of interfacial magnetism. Nat Mater 14:174
20. Vaz CAF, Hoffman J, Ahn CH, Ramesh R (2010) Magnetoelectric coupling effects in multiferroic complex oxide composite structures. Adv Mater 22:2900
21. Ma J, Hu J, Li Z, Nan C-W (2011) Recent progress in multiferroic magnetoelectric composites: from bulk to thin films. Adv Mater 23(1062)
22. Vaz CAF (2012) Electric field control of magnetism in multiferroic heterostructures. J Phys Condens Matter 24:333201
23. Zheng H, Wang J, Lofland SE, Ma Z, Mohaddes-Ardabili L, Zhao T, Salamanca-Riba L, Shinde SR, Ogale SB, Bai F, Viehland D, Jia Y, Schlom DG, Wuttig M, Roytburd A, Ramesh R (2004) Multiferroic $BaTiO_3$-$CoFe_2O_4$ nanostructures. Science 303:661
24. Li J, Levin I, Slutsker J, Provenzano V, Schenck PK, Ramesh R, Ouyang J, Roytburd AL (2005) Self-assembled multiferroic nanostructures in the $CoFe_2O_4$-$PbTiO_3$ system. Appl Phys Lett 87:072909

25. Zavaliche F, Zheng H, Mohaddes-Ardabili L, Yang SY, Zhan Q, Shafer P, Reilly E, Chopdekar R, Jia Y, Wright P, Schlom DG, Suzuki Y, Ramesh R (2005) Electric field-induced magnetization switching in epitaxial columnar nanostructures. Nano Lett 5:1793
26. Levin I, Li J, Slutsker J, Roytburd AL (2006) Design of self-assembled multiferroic nanostructures in epitaxial films. Adv Mater 18:2044
27. Zheng H, Straub F, Zhan Q, Yang P-L, Hsieh W-K, Zavaliche F, Chu Y-H, Dahmen U, Ramesh R (2006) Self-assembled growth of $BiFeO_3$-$CoFe_2O_4$ nanostructures. Adv Mater 18:2747
28. Zhan Q, Yu R, Crane SP, Zheng H, Kisielowski C, Ramesh R (2006) Structure and interface chemistry of perovskite-spinel nanocomposite thin films. Appl Phys Lett 89:172902
29. Slutsker J, Levin I, Li J, Artemev A, Roytburd AL (2006) Effect of elastic interactions on the self-assembly of multiferroic nanostructures in epitaxial films. Phys Rev B 73:184127
30. Dix N, Muralidharan R, Guyonnet J, Warot-Fonrose B, Varela M, Paruch P, Sánchez F, Fontcuberta J (2009) On the strain coupling across vertical interfaces of switchable $BiFeO_3$-$CoFe_2O_4$ multiferroic nanostructures. Appl Phys Lett 95:062907
31. Weal E, Patnaik S, Bi Z, Wang H, Fix T, Kursumovic A, Driscoll JLM (2010) Coexistence of strong ferromagnetism and polar switching at room temperature in Fe_3O_4-$BiFeO_3$ nanocomposite thin films. Appl Phys Lett 97:153121
32. Aimon NM, Hun Kim D, Kyoon Choi H, Ross CA (2012) Deposition of epitaxial $BiFeO_3$/$CoFe_2O_4$ nanocomposites on (001) $SrTiO_3$ by combinatorial pulsed laser deposition. Appl Phys Lett 100:092901
33. Kim DH, Aimon NM, Sun X, Ross CA (2014) Compositionally modulated magnetic epitaxial spinel/perovskite nanocomposite thin films. Adv Funct Mater 24:2334
34. Kim DH, Aimon NM, Sun XY, Kornblum L, Walker FJ, Ahn CH, Ross CA (2014) Integration of self-assembled epitaxial $BiFeO_3$-$CoFe_2O_4$ multiferroic nanocomposites on silicon substrates. Adv Funct Mater 24:5889
35. Gao X, Rodriguez BJ, Liu L, Birajdar B, Pantel D, Ziese M, Alexe M, Hesse D (2010) Microstructure and properties of well-ordered multiferroic Pb(Zr, Ti)O_3/$CoFe_2O_4$ nanocomposites. ACS Nano 4:1099
36. Vrejoiu I, Morelli A, Biggemann D, Pippel E (2011) Ordered arrays of multiferroic epitaxial nanostructures. Nano Rev 2:7364
37. Vrejoiu I, Preziosi D, Morelli A, Pippel E (2012) Multiferroic $PbZr_xTi_{1-x}O_3$/Fe_3O_4 epitaxial sub-micron sized structures. Appl Phys Lett 100:102903
38. Choi HK, Aimon NM, Kim DH, Sun XY, Gwyther J, Manners I, Ross CA (2014) Hierarchical templating of a $BiFeO_3$-$CoFe_2O_4$ multiferroic nanocomposite by a triblock terpolymer film. ACS Nano 8:9248
39. Allwood DA, Xiong G, Faulkner CC, Atkinson D, Petit D, Cowburn RP (2005) Magnetic domain-wall logic. Science 309:1688
40. Parkin SSP, Hayashi M, Thomas L (2008) Magnetic domain-wall racetrack memory. Science 320:190
41. Binek C, Doudin B (2005) Magnetoelectronics with magnetoelectrics. J Phys Condens Matter 17:L39
42. Bibes M, Barthélémy A (2008) Multiferroics: towards a magnetoelectric memory. Nat Mater 7:425
43. Hu J-M, Li Z, Chen L-Q, Nan C-W (2011) High-density magnetoresistive random access memory operating at ultralow voltage at room temperature. Nat Commun 2:553
44. Hu J-M, Li Z, Chen L-Q, Nan C-W (2012) Design of a voltage-controlled magnetic random access memory based on anisotropic magnetoresistance in a single magnetic layer. Adv Mater 24:2869
45. Gajek M, Bibes M, Fusil S, Bouzehouane K, Fontcuberta J, Barthélémy A, Fert A (2007) Tunnel junctions with multiferroic barriers. Nat Mater 6:296
46. Scott JF (2007) Data storage: multiferroic memories. Nat Mater 6:256

47. Velev JP, Duan C-G, Burton JD, Smogunov A, Niranjan MK, Tosatti E, Jaswal SS, Tsymbal EY (2009) Magnetic tunnel junctions with ferroelectric barriers: prediction of four resistance states from first principles. Nano Lett 9:427
48. Garcia V, Bibes M, Bocher L, Valencia S, Kronast F, Crassous A, Moya X, Enouz-Vedrenne-S, Gloter A, Imhoff D, Deranlot C, Mathur ND, Fusil S, Bouzehouane K, Barthélémy A (2010) Ferroelectric control of spin polarization. Science 327:1106
49. Pantel D, Goetze S, Hesse D, Alexe M (2012) Reversible electrical switching of spin polarization in multiferroic tunnel junctions. Nat Mater 11:289
50. Lou J, Liu M, Reed D, Ren Y, Sun NX (2009) Giant electric field tuning of magnetism in novel multiferroic FeGaB/Lead Zinc Niobate-Lead Titanate (PZN-PT) heterostructures. Adv Mater 21:4711
51. Liu M, Obi O, Lou J, Chen Y, Cai Z, Stoute S, Espanol M, Lew M, Situ X, Ziemer KS, Harris VG, Sun NX (2009) Giant electric field tuning of magnetic properties in multiferroic ferrite/ferroelectric heterostructures. Adv Funct Mater 19:1826
52. Liu M, Howe BM, Grazulis L, Mahalingam K, Nan T, Sun NX, Brown GJ (2013) Voltage-impulse-induced non-volatile ferroelastic switching of ferromagnetic resonance for reconfigurable magnetoelectric microwave devices. Adv Mater 25:4886
53. Duan C-G, Jaswal SS, Tsymbal EY (2006) Predicted magnetoelectric effect in Fe/$BaTiO_3$ multilayers: ferroelectric control of magnetism. Phys Rev Lett 97:047201
54. Weisheit M, Fähler S, Marty A, Souche Y, Poinsignon C, Givord D (2007) Electric field induced modification of magnetism in thin-film ferromagnets. Science 315:349
55. Yamauchi K, Sanyal B, Picozzi S (2007) Interface effects at a half-metal/ferroelectric junction. Appl Phys Lett 91:062506
56. Fechner M, Maznichenko IV, Ostanin S, Ernst A, Henk J, Bruno P, Mertig I (2008) Magnetic phase transition in two-phase multiferroics predicted from first principles. Phys Rev B 78:212406
57. Niranjan MK, Velev JP, Duan C-G, Jaswal SS, Tsymbal EY (2008) Magnetoelectric effect at the Fe_3O_4/$BaTiO_3$ (001) interface: a first-principles study. Phys Rev B 78:104405
58. Duan C-G, Velev JP, Sabirianov RF, Zhu Z, Chu J, Jaswal SS, Tsymbal EY (2008) Surface magnetoelectric effect in ferromagnetic metal films. Phys Rev Lett 101:137201
59. Duan C-G, Velev JP, Sabirianov RF, Mei WN, Jaswal SS, Tsymbal EY (2008) Tailoring magnetic anisotropy at the ferromagnetic/ferroelectric interface. Appl Phys Lett 92:122905
60. Nakamura K, Shimabukuro R, Fujiwara Y, Akiyama T, Ito T, Freeman AJ (2009) Giant modification of the magnetocrystalline anisotropy in transition-metal monolayers by an external electric field. Phys Rev Lett 102:187201
61. Tsujikawa M, Oda T (2009) Finite electric field effects in the large perpendicular magnetic anisotropy surface Pt/Fe/Pt(001): a first-principles study. Phys Rev Lett 102:247203
62. Lee J, Sai N, Cai T, Niu Q, Demkov AA (2010) Interfacial magnetoelectric coupling in tricomponent superlattices. Phys Rev B 81:144425
63. Meyerheim HL, Klimenta F, Ernst A, Mohseni K, Ostanin S, Fechner M, Parihar S, Maznichenko IV, Mertig I, Kirschner J (2011) Structural secrets of multiferroic interfaces. Phys Rev Lett 106:087203
64. Bocher L, Gloter A, Crassous A, Garcia V, March K, Zobelli A, Valencia S, Enouz-Vedrenne S, Moya X, Marthur ND, Deranlot C, Fusil S, Bouzehouane K, Bibes M, Barthélémy A, Colliex C, Stéphan O (2012) Atomic and electronic structure of the $BaTiO_3$/Fe interface in multiferroic tunnel junctions. Nano Lett 12:376
65. Borek S, Maznichenko IV, Fischer G, Hergert W, Mertig I, Ernst A, Ostanin S, Chassé A (2012) First-principles calculation of x-ray absorption spectra and x-ray magnetic circular dichroism of ultrathin Fe films on $BaTiO_3$(001). Phys Rev B 85:134432
66. Dai J-Q, Song Y-M, Zhang H (2012) Enhancement of magnetoelectric effect by combining different interfacial coupling mechanisms. J Appl Phys 111:114301
67. Borisov VS, Ostanin S, Maznichenko IV, Ernst A, Mertig I (2014) Magnetoelectric properties of the Co/$PbZr_xTi_{1-x}O_3$ (001) interface studied from first principles. Phys Rev B 89:054436

68. Radaelli G, Petti D, Plekhanov E, Fina I, Torelli P, Salles BR, Cantoni M, Rinaldi C, Gutiérrez D, Panaccione G, Varela M, Picozzi S, Fontcuberta J, Bertacco R (2014) Electric control of magnetism at the Fe/$BaTiO_3$ interface. Nat Commun 5:3404
69. Brovko OO, Ruiz-Daz P, Dasa TR, Stepanyuk VS (2014) Controlling magnetism on metal surfaces with non-magnetic means: electric fields and surface charging. J Phys Condens Matter 26:093001
70. Burton JD, Tsymbal EY (2009) Prediction of electrically induced magnetic reconstruction at the manganite/ferroelectric interface. Phys Rev B 80:174406
71. Burton JD, Tsymbal EY (2011) Giant tunneling electroresistance effect driven by an electrically controlled spin valve at a complex oxide interface. Phys Rev Lett 106:157203
72. Dong S, Dagotto E (2013) Full control of magnetism in a manganite bilayer by ferroelectric polarization. Phys Rev B 88:140404
73. Chen H, Qiao Q, Marshall MSJ, Georgescu AB, Gulec A, Phillips PJ, Klie RF, Walker FJ, Ahn CH, Ismail-Beigi S (2014) Reversible modulation of orbital occupations via an interface-induced polar state in metallic manganites. Nano Lett 14:4965
74. Hong X, Posadas A, Lin A, Ahn CH (2003) Ferroelectric-field-induced tuning of magnetism in the colossal magnetoresistive oxide $La_{1-x}Sr_xMnO_3$. Phys Rev B 68:134415
75. Hong X, Posadas A, Ahn CH (2005) Examining the screening limit of field effect devices via the metal-insulator transition. Appl Phys Lett 86:142501
76. Kanki T, Tanaka H, Kawai T (2006) Electric control of room temperature ferromagnetism in a $Pb(Zr_{0.2}Ti_{0.8})O_3/La_{0.85}Ba_{0.15}MnO_3$ field-effect transistor. Appl Phys Lett 89:242506
77. Molegraaf HJA, Hoffman J, Vaz CAF, Gariglio S, van der Marel D, Ahn CH, Triscone J-M (2009) Magnetoelectric effects in complex oxides with competing ground states. Adv Mater 21:3470
78. Dhoot AS, Israel C, Moya X, Mathur ND, Friend RH (2009) Large electric field effect in electrolyte-gated manganites. Phys Rev Lett 102:136402
79. Vaz CAF, Hoffman J, Segal Y, Reiner JW, Grober RD, Zhang Z, Ahn CH, Walker FJ (2010) Origin of the magnetoelectric coupling effect in $Pb(Zr_{0.2}Ti_{0.8})O_3/La_{0.8}Sr_{0.2}MnO_3$ multiferroic heterostructures. Phys Rev Lett 104:127202
80. Vaz CAF, Segal Y, Hoffman J, Grober RD, Walker FJ, Ahn CH (2010) Temperature dependence of the magnetoelectric effect in $Pb(Zr_{0.2}Ti_{0.8})O_3/La_{0.8}Sr_{0.2}MnO_3$ multiferroic heterostructures. Appl Phys Lett 97:042506
81. Brivio S, Cantoni M, Petti D, Bertacco R (2010) Near-room-temperature control of magnetization in field effect devices based on $La_{0.67}Sr_{0.33}MnO_3$ thin films. J Appl Phys 108:113906
82. Dong S, Zhang X, Yu R, Liu J-M, Dagotto E (2011) Microscopic model for the ferroelectric field effect in oxide heterostructures. Phys Rev B 84:155117
83. Chen H, Ismail-Beigi S (2012) Ferroelectric control of magnetization in $La_{1-x}Sr_xMnO_3$ manganites: a first-principles study. Phys Rev B 86:024433
84. Lu H, George TA, Wang Y, Ketsman I, Burton JD, Bark C-W, Ryu S, Kim DJ, Wang J, Binek C, Dowben PA, Sokolov A, Eom C-B, Tsymbal EY, Gruverman A (2012) Electric modulation of magnetization at the $BaTiO_3/La_{0.67}Sr_{0.33}MnO_3$ interfaces. Appl Phys Lett 100:232904
85. Yin YW, Burton JD, Kim Y-M, Borisevich AY, Pennycook SJ, Yang SM, Noh TW, Gruverman A, Li XG, Tsymbal EY, Li Q (2013) Enhanced tunnelling electroresistance effect due to a ferroelectrically induced phase transition at a magnetic complex oxide interface. Nat Mater 12:397
86. Jiang L, Choi WS, Jeen H, Dong S, Kim Y, Han M-G, Zhu Y, Kalinin SV, Dagotto E, Egami T, Lee HN (2013) Tunneling electroresistance induced by interfacial phase transitions in ultrathin oxide heterostructures. Nano Lett 13:5837
87. Yi D, Liu J, Okamoto S, Jagannatha S, Chen Y-C, Yu P, Chu Y-H, Arenholz E, Ramesh R (2013) Tuning the competition between ferromagnetism and antiferromagnetism in a half-doped manganite through magnetoelectric coupling. Phys Rev Lett 111:127601

88. Leufke PM, Kruk R, Brand RA, Hahn H (2013) In situ magnetometry studies of magneto-electric LSMO/PZT heterostructures. Phys Rev B 87:094416
89. Preziosi D, Fina I, Pippel E, Hesse D, Marti X, Bern F, Ziese M, Alexe M (2014) Tailoring the interfacial magnetic anisotropy in multiferroic field-effect devices. Phys Rev B 90:125155
90. Ma X, Kumar A, Dussan S, Zhai H, Fang F, Zhao HB, Scott JF, Katiyar RS, Lüpke G (2014) Charge control of antiferromagnetism at $PbZr_{0.52}Ti_{0.48}O_3/La_{0.67}Sr_{0.33}MnO_3$ interface. Appl Phys Lett 104:132905
91. Kim Y-M, Morozovska A, Eliseev E, Oxley MP, Mishra R, Selbach SM, Grande T, Pantelides ST, Kalinin SV, Borisevich AY (2014) Direct observation of ferroelectric field effect and vacancy-controlled screening at the $BiFeO_3/La_xSr_{1-x}MnO_3$ interface. Nat Mater 13:1019
92. Ohno H, Chiba D, Matsukura F, Omiya T, Abe E, Dietl T, Ohno Y, Ohtani K (2000) Electric-field control of ferromagnetism. Nature 408:944
93. Park YD, Hanbicki AT, Erwin SC, Hellberg CS, Sullivan JM, Mattson JE, Ambrose TF, Wilson A, Spanos G, Jonker BT (2002) A group-IV ferromagnetic semiconductor: Mn_xGe_{1-x}. Science 295:651
94. Chiba D, Yamanouchi M, Matsukura F, Ohno H (2003) Electrical manipulation of magnetization reversal in a ferromagnetic semiconductor. Science 301:943
95. Kneip MK, Yakovlev DR, Bayer M, Slobodskyy T, Schmidt G, Molenkamp LW (2006) Electric field control of magnetization dynamics in ZnMnSe/ZnBeSe diluted-magnetic semiconductor heterostructures. Appl Phys Lett 88:212105
96. Stolichnov I, Riester SWE, Trodahl HJ, Setter N, Rushforth AW, Edmonds KW, Campion RP, Foxon CT, Gallagher BL, Jungwirth T (2008) Non-volatile ferroelectric control of ferromagnetism in (Ga, Mn)As. Nat Mater 7:464
97. Chiba D, Sawicki M, Nishitani Y, Nakatani Y, Matsukura F, Ohno H (2008) Magnetization vector manipulation by electric fields. Nature 455:515
98. Riester SWE, Stolichnov I, Trodahl HJ, Setter N, Rushforth AW, Edmonds KW, Campion RP, Foxon CT, Gallagher BL, Jungwirth T (2009) Toward a low-voltage multiferroic transistor: magnetic (Ga, Mn)As under ferroelectric control. Appl Phys Lett 94:063504
99. Endo M, Chiba D, Shimotani H, Matsukura F, Iwasa Y, Ohno H (2010) Electric double layer transistor with a (Ga, Mn)As channel. Appl Phys Lett 96:022515
100. Stolichnov I, Riester SWE, Mikheev E, Setter N, Rushforth AW, Edmonds KW, Campion RP, Foxon CT, Gallagher BL, Jungwirth T, Trodahl HJ (2011) Enhanced Curie temperature and nonvolatile switching of ferromagnetism in ultrathin (Ga, Mn)As channels. Phys Rev B 83:115203
101. Mikheev E, Stolichnov I, De Ranieri E, Wunderlich J, Trodahl HJ, Rushforth AW, Riester SWE, Campion RP, Edmonds KW, Gallagher BL, Setter N (2012) Magnetic domain wall propagation under ferroelectric control. Phys Rev B 86:235130
102. Tokura Y (2006) Critical features of colossal magnetoresistive manganites. Rep Prog Phys 69:797
103. Nogués J, Schuller IK (1999) Exchange bias. J Magn Magn Mater 192:203
104. Berkowitz AE, Takano K (1999) Exchange anisotropy – a review. J Magn Magn Mater 200:552
105. Laukhin V, Skumryev V, Martí X, Hrabovsky D, Sánchez F, García-Cuenca MV, Ferrater C, Varela M, Lüders U, Bobo JF, Fontcuberta J (2006) Electric-field control of exchange bias in multiferroic epitaxial heterostructures. Phys Rev Lett 97:227201
106. Skumryev V, Laukhin V, Fina I, Martí X, Sánchez F, Gospodinov M, Fontcuberta J (2011) Magnetization reversal by electric-field decoupling of magnetic and ferroelectric domain walls in multiferroic-based heterostructures. Phys Rev Lett 106:057206
107. Chu Y-H, Martin LW, Holcomb MB, Gajek M, Han S-J, He Q, Balke N, Yang C-H, Lee D, Hu W, Zhan Q, Yang P-L, Fraile-Rodríguez A, Scholl A, Wang SX, Ramesh R (2008)

Electric-field control of local ferromagnetism using a magnetoelectric multiferroic. Nat Mater 7:478
108. Martin LW, Chu Y-H, Holcomb MB, Huijben M, Yu P, Han S-J, Lee D, Wang SX, Ramesh R (2008) Nanoscale control of exchange bias with $BiFeO_3$ thin films. Nano Lett 8:2050
109. Béa H, Bibes M, Ott F, Dupé B, Zhu X-H, Petit S, Fusil S, Deranlot C, Bouzehouane K, Barthélémy A (2008) Mechanisms of exchange bias with multiferroic $BiFeO_3$ epitaxial thin films. Phys Rev Lett 100:017204
110. Lebeugle D, Mougin A, Viret M, Colson D, Ranno L (2009) Electric field switching of the magnetic anisotropy of a ferromagnetic layer exchange coupled to the multiferroic compound $BiFeO_3$. Phys Rev Lett 103:257601
111. Wu SM, Cybart SA, Yu P, Rossell MD, Zhang JX, Ramesh R, Dynes RC (2010) Reversible electric control of exchange bias in a multiferroic field-effect device. Nat Mater 9:756
112. Lebeugle D, Mougin A, Viret M, Colson D, Allibe J, Béa H, Jacquet E, Deranlot C, Bibes M, Barthélémy A (2010) Exchange coupling with the multiferroic compound $BiFeO_3$ in antiferromagnetic multidomain films and single-domain crystals. Phys Rev B 81:134411
113. Heron JT, Trassin M, Ashraf K, Gajek M, He Q, Yang SY, Nikonov DE, Chu Y-H, Salahuddin S, Ramesh R (2011) Electric-field-induced magnetization reversal in a ferromagnet-multiferroic heterostructure. Phys Rev Lett 107:217202
114. Allibe J, Fusil S, Bouzehouane K, Daumont C, Sando D, Jacquet E, Deranlot C, Bibes M, Barthélémy A (2012) Room temperature electrical manipulation of giant magnetoresistance in spin valves exchange-biased with $BiFeO_3$. Nano Lett 12:1141
115. Trassin M, Clarkson JD, Bowden SR, Liu J, Heron JT, Paull RJ, Arenholz E, Pierce DT, Unguris J (2013) Interfacial coupling in multiferroic/ferromagnet heterostructures. Phys Rev B 87:134426
116. Heron JT, Bosse JL, He Q, Gao Y, Trassin M, Ye L, Clarkson JD, Wang C, Liu J, Salahuddin S et al (2014) Deterministic switching of ferromagnetism at room temperature using an electric field. Nature 516:370
117. Heron JT, Schlom DG, Ramesh R (2014) Electric field control of magnetism using $BiFeO_3$-based heterostructures. Appl Phys Rev 1:021303
118. Hochstrat A, Binek C, Chen X, Kleemann W (2004) Extrinsic control of the exchange bias. J Magn Magn Mater 272:325
119. Borisov P, Hochstrat A, Chen X, Kleemann W, Binek C (2005) Magnetoelectric switching of exchange bias. Phys Rev Lett 94:117203
120. He X, Wang Y, Wu N, Caruso AN, Vescovo E, Belashchenko KD, Dowben PA, Binek C (2010) Robust isothermal electric control of exchange bias at room temperature. Nat Mater 9:579
121. Thiele C, Dörr K, Fähler S, Schultz L, Meyer DC, Levin AA, Paufler P (2005) Voltage controlled epitaxial strain in $La_{0.7}Sr_{0.3}MnO_3/Pb(Mg_{1/3}Nb_{2/3})O_3$-$PbTiO_3$(001) films. Appl Phys Lett 87:262502
122. Thiele C, Dörr K, Bilani O, Rödel J, Schultz L (2007) Influence of strain on the magnetization and magnetoelectric effect in $La_{0.7}A_{0.3}MnO_3$/PMN-PT(001) (A=Sr,Ca). Phys Rev B 75:054408
123. Zheng RK, Wang Y, Chan HLW, Choy CL, Luo HS (2007) Determination of the strain dependence of resistance in $La_{0.7}Sr_{0.3}MnO_3$/PMN-PT using the converse piezoelectric effect. Phys Rev B 75:212102
124. Wang J, Hu FX, Li RW, Sun JR, Shen BG (2010) Strong tensile strain induced charge/orbital ordering in (001)-$La_{7/8}Sr_{1/8}MnO_3$ thin film on $0.7Pb(Mg_{1/3}Nb_{2/3})O_3$-$0.3PbTiO_3$. Appl Phys Lett 96:052501
125. Kim J-Y, Yao L, van Dijken S (2013) Coherent piezoelectric strain transfer to thick epitaxial ferromagnetic films with large lattice mismatch. J Phys Condens Matter 25:082205

126. Sheng ZG, Gao J, Sun YP (2009) Coaction of electric field induced strain and polarization effects in $La_{0.7}Ca_{0.3}MnO_3$/PMN-PT structures. Phys Rev B 79:174437
127. Rata AD, Herklotz A, Nenkov K, Schultz L, Dörr K (2008) Strain-induced insulator state and giant gauge factor of $La_{0.7}Sr_{0.3}CoO_3$ films. Phys Rev Lett 100:076401
128. Zheng RK, Jiang Y, Wang Y, Chan HLW, Choy CL, Luo HS (2009) Ferroelectric poling and converse-piezoelectric-effect-induced strain effects in $La_{0.7}Ba_{0.3}MnO_3$ thin films grown on ferroelectric single-crystal substrates. Phys Rev B 79:174420
129. Biegalski MD, Dörr K, Kim DH, Christen HM (2010) Applying uniform reversible strain to epitaxial oxide films. Appl Phys Lett 96:151905
130. Li F, Zhang S, Xu Z, Wei X, Luo J, Shrout TR (2010) Composition and phase dependence of the intrinsic and extrinsic piezoelectric activity of domain engineered (1-x)$Pb(Mg_{1/3}Nb_{2/3})O_{3-x}PbTiO_3$ crystals. J Appl Phys 108:034106
131. Yang JJ, Zhao YG, Tian HF, Luo LB, Zhang HY, He YJ, Luo HS (2009) Electric field manipulation of magnetization at room temperature in multiferroic $CoFe_2O_4/Pb(Mg_{1/3}Nb_{2/3})0.7Ti_{0.3}O_3$ heterostructures. Appl Phys Lett 94:212504
132. Park JH, Lee J-H, Kim MG, Jeong YK, Oak M-A, Jang HM, Choi HJ, Scott JF (2010) In-plane strain control of the magnetic remanence and cation-charge redistribution in $CoFe_2O_4$ thin film grown on a piezoelectric substrate. Phys Rev B 81:134401
133. Park JH, Jeong YK, Ryu S, Son JY, Jang HM (2010) Electric-field-control of magnetic remanence of $NiFe_2O_4$ thin film epitaxially grown on $Pb(Mg_{1/3}Nb_{2/3})O_3$-$PbTiO_3$. Appl Phys Lett 96:192504
134. Yang Y, Luo ZL, Huang H, Gao Y, Bao J, Li XG, Zhang S, Zhao YG, Chen X, Pan G, Gao C (2011) Electric-field-control of resistance and magnetization switching in multiferroic $Zn_{0.4}Fe_{0.6}O_4$/0.7$Pb(Mg_{2/3}Nb_{1/3})O_3$-0.3$PbTiO_3$ epitaxial heterostructures. Appl Phys Lett 98:153509
135. Wang Z, Wang Y, Ge W, Li J, Viehland D (2013) Volatile and nonvolatile magnetic easy axis rotation in epitaxial ferromagnetic thin films on ferroelectric single crystal substrates. Appl Phys Lett 103:132909
136. Kim J-H, Ryu K-S, Jeong J-W, Shin S-C (2010) Large converse magnetoelectric coupling effect at room temperature in CoPd/PMN-PT (001) heterostructure. Appl Phys Lett 97:252508
137. Wu T, Bur A, Wong K, Zhao P, Lynch CS, Amiri PK, Wang KL, Carman GP (2011) Electrical control of reversible and permanent magnetization reorientation for magnetoelectric memory devices. Appl Phys Lett 98:262504
138. Hsu C-J, Hockel JL, Carman GP (2012) Magnetoelectric manipulation of domain wall configuration in thin film $Ni/[Pb(Mn_{1/3}Nb_{2/3})O_3]0.68$-$[PbTiO_3]0.32$ (001) heterostructure. Appl Phys Lett 100:092902
139. Yang S-W, Peng R-C, Jiang T, Liu Y-K, Feng L, Wang J-J, Chen L-Q, Li X-G, Nan C-W (2014) Non-volatile 180° magnetization reversal by an electric field in multiferroic heterostructures. Adv Mater 26:7091
140. Brandlmaier A, Geprägs S, Weiler M, Boger A, Opel M, Huebl H, Bihler C, Brandt MS, Botters B, Grundler D, Gross R, Goennenwein STB (2008) In situ manipulation of magnetic anisotropy in magnetite thin films. Phys Rev B 77:104445
141. Bihler C, Althammer M, Brandlmaier A, Geprägs S, Weiler M, Opel M, Schoch W, Limmer W, Gross R, Brandt MS, Goennenwein STB (2008) $Ga_{1-x}Mn_xAs$/piezoelectric actuator hybrids: a model system for magnetoelastic magnetization manipulation. Phys Rev B 78:045203
142. Tiercelin N, Dusch Y, Klimov A, Giordano S, Preobrazhensky V, Pernod P (2011) Room temperature magnetoelectric memory cell using stress-mediated magnetoelastic switching in nanostructured multilayers. Appl Phys Lett 99:192507
143. Brandlmaier A, Geprägs S, Woltersdorf G, Gross R, Goennenwein STB (2011) Nonvolatile, reversible electric-field controlled switching of remanent magnetization in multifunctional ferromagnetic/ferroelectric hybrids. J Appl Phys 110:043913

144. Parkes DE, Cavill SA, Hindmarch AT, Wadley P, McGee F, Staddon CR, Edmonds KW, Campion RP, Gallagher BL, Rushforth AW (2012) Non-volatile voltage control of magnetization and magnetic domain walls in magnetostrictive epitaxial thin films. Appl Phys Lett 101:072402
145. Brandlmaier A, Brasse M, Geprägs S, Weiler M, Gross R, Goennenwein STB (2012) Magneto-optical imaging of elastic strain-controlled magnetization reorientation. Eur Phys J B 85:124
146. Cavill SA, Parkes DE, Miguel J, Dhesi SS, Edmonds KW, Campion RP, Rushforth AW (2013) Electrical control of magnetic reversal processes in magnetostrictive structures. Appl Phys Lett 102:032405
147. Xi L, Guo X, Wang Z, Li Y, Yao Y, Zuo Y, Xue D (2013) Voltage-driven in-plane magnetization easy axis switching in FeNi/piezoelectric actuator hybrid structure. Appl Phys Express 6:015804
148. Pertsev NA (2008) Giant magnetoelectric effect via strain-induced spin reorientation transitions in ferromagnetic films. Phys Rev B 78:212102
149. Hu J-M, Nan CW (2009) Electric-field-induced magnetic easy-axis reorientation in ferromagnetic/ferroelectric layered heterostructures. Phys Rev B 80:224416
150. Pertsev NA, Kohlstedt H (2010) Resistive switching via the converse magnetoelectric effect in ferromagnetic multilayers on ferroelectric substrates. Nanotechnology 21:475202
151. Hu J-M, Li Z, Wang J, Nan CW (2010) Electric-field control of strain-mediated magnetoelectric random access memory. J Appl Phys 107:093912
152. Liu M, Lou J, Li S, Sun NX (2011) E-field control of exchange bias and deterministic magnetization switching in AFM/FM/FE multiferroic heterostructures. Adv Funct Mater 21:2593
153. Ghidini M, Pellicelli R, Prieto JL, Moya X, Soussi J, Briscoe J, Dunn S, Mathur ND (2013) Non-volatile electrically-driven repeatable magnetization reversal with no applied magnetic field. Nat Commun 4:1453
154. Liu M, Zhou Z, Nan T, Howe BM, Brown GJ, Sun NX (2013) Voltage tuning of ferromagnetic resonance with bistable magnetization switching in energy-efficient magnetoelectric composites. Adv Mater 25:1435
155. Chung T-K, Carman GP, Mohanchandra KP (2008) Reversible magnetic domain-wall motion under an electric field in a magnetoelectric thin film. Appl Phys Lett 92:112509
156. Dean J, Bryan MT, Schrefl T, Allwood DA (2011) Stress-based control of magnetic nanowire domain walls in artificial multiferroic systems. J Appl Phys 109:023915
157. Lei N, Devolder T, Agnus G, Aubert P, Daniel L, Kim J-V, Zhao W, Trypiniotis T, Cowburn RP, Chappert C, Ravelosona D, Lecoeur P (2013) Strain-controlled magnetic domain wall propagation in hybrid piezoelectric/ferromagnetic structures. Nat Commun 4:1378
158. de Ranieri E, Roy PE, Fang D, Vehsthedt EK, Irvine AC, Heiss D, Casiraghi A, Campion RP, Gallagher BL, Jungwirth T, Wunderlich J (2013) Piezoelectric control of the mobility of a domain wall driven by adiabatic and non-adiabatic torques. Nat Mater 12:808
159. Lemerle S, Ferré J, Chappert C, Mathet V, Giamarchi T, Le Doussal P (1998) Domain wall creep in an Ising ultrathin magnetic film. Phys Rev Lett 80:849
160. Glazer AM, Mabud SA (1978) Powder profile refinement of lead zirconate titanate at several temperatures. II. Pure $PbTiO_3$. Acta Crystallogr B 34:1065
161. Kwei GH, Lawson AC, Billinge SJL, Cheong SW (1993) Structures of the ferroelectric phases of barium titanate. J Phys Chem 97:2368
162. Kay HF, Vousden P (1949) Symmetry changes in barium titanate at low temperatures and their relation to its ferroelectric properties. Philos Mag 40:1019
163. Lee MK, Nath TK, Eom CB, Smoak MC, Tsui F (2000) Strain modification of epitaxial perovskite oxide thin films using structural transitions of ferroelectric $BaTiO_3$ substrate. Appl Phys Lett 77:3547

164. Eerenstein W, Wiora M, Prieto JL, Scott JF, Mathur ND (2007) Giant sharp and persistent converse magnetoelectric effects in multiferroic epitaxial heterostructures. Nat Mater 6:348
165. Alberca A, Munuera C, Tornos J, Mompean FJ, Biskup N, Ruiz A, Nemes NM, de Andres A, León C, Santamaría J, García-Hernández M (2012) Ferroelectric substrate effects on the magnetism, magnetotransport, and electroresistance of $La_{0.7}Ca_{0.3}MnO_3$ thin films on $BaTiO_3$. Phys Rev B 86:144416
166. Tian HF, Qu TL, Luo LB, Yang JJ, Guo SM, Zhang HY, Zhao YG, Li JQ (2008) Strain induced magnetoelectric coupling between magnetite and $BaTiO_3$. Appl Phys Lett 92:063507
167. Vaz CAF, Hoffman J, Posadas A-B, Ahn CH (2009) Magnetic anisotropy modulation of magnetite in Fe_3O_4/$BaTiO_3$(100) epitaxial structures. Appl Phys Lett 94:022504
168. Sterbinsky GE, Wessels BW, Kim J-W, Karapetrova E, Ryan PJ, Keavney DJ (2010) Strain-driven spin reorientation in magnetite/barium titanate heterostructures. Appl Phys Lett 96:092510
169. Sahoo S, Polisetty S, Duan C-G, Jaswal SS, Tsymbal EY, Binek C (2007) Ferroelectric control of magnetism in $BaTiO_3$/Fe heterostructures via interface strain coupling. Phys Rev B 76:092108
170. Taniyama T, Akasaka K, Fu D, Itoh M (2009) Artificially controlled magnetic domain structures in ferromagnetic dots/ferroelectric heterostructures. J Appl Phys 105:070000
171. Brivio S, Petti D, Bertacco R, Cezar JC (2011) Electric field control of magnetic anisotropies and magnetic coercivity in Fe/$BaTiO_3$(001) heterostructures. Appl Phys Lett 98:092505
172. Shirahata Y, Nozaki T, Venkataiah G, Taniguchi H, Itoh M, Taniyama T (2011) Switching of the symmetry of magnetic anisotropy in Fe/$BaTiO_3$ heterostructures. Appl Phys Lett 99:022501
173. Venkataiah G, Shirahata Y, Itoh M, Taniyama T (2011) Manipulation of magnetic coercivity of Fe film in Fe/$BaTiO_3$ heterostructure by electric field. Appl Phys Lett 99:102506
174. Venkataiah G, Shirahata Y, Suzuki I, Itoh M, Taniyama T (2012) Strain-induced reversible and irreversible magnetization switching in Fe/$BaTiO_3$ heterostructures. J Appl Phys 111:033921
175. Czeschka FD, Geprägs S, Opel M, Goennenwein STB, Gross R (2009) Giant magnetic anisotropy changes in Sr_2CrReO_6 thin films on $BaTiO_3$. Appl Phys Lett 95:062508
176. Pan M, Hong S, Guest JR, Liu Y, Petford-Long A (2013) Visualization of magnetic domain structure changes induced by interfacial strain in $CoFe_2O_4$/$BaTiO_3$ heterostructures. J Phys D Appl Phys 46:055001
177. Moubah R, Magnus F, Hjörvarsson B, Andersson G (2014) Strain enhanced magnetic anisotropy in SmCo/$BaTiO_3$ multiferroic heterostructures. J Appl Phys 115:053905
178. Polisetty S, Echtenkamp W, Jones K, He X, Sahoo S, Binek C (2010) Piezoelectric tuning of exchange bias in a $BaTiO_3$/Co/CoO heterostructure. Phys Rev B 82:134419
179. Lahtinen THE, van Dijken S (2013) Temperature control of local magnetic anisotropy in multiferroic CoFe/$BaTiO_3$. Appl Phys Lett 102:112406
180. Taniyama T, Akasaka K, Fu D, Itoh M, Takashima H, Prijamboedi B (2007) Electrical voltage manipulation of ferromagnetic microdomain structures in a ferromagnetic/ferroelectric hybrid structure. J Appl Phys 101:09F512
181. Geprägs S, Brandlmaier A, Opel M, Gross R, Goennenwein STB (2010) Electric field controlled manipulation of the magnetization in Ni/$BaTiO_3$ hybrid structures. Appl Phys Lett 96:142509
182. Lahtinen THE, Tuomi JO, van Dijken S (2011) Pattern transfer and electric-field-induced magnetic domain formation in multiferroic heterostructures. Adv Mater 23:3187
183. Lahtinen THE, Tuomi JO, van Dijken S (2011) Electrical writing of magnetic domain patterns in ferromagnetic/ferroelectric heterostructures. IEEE Trans Magn 47:3768
184. Lahtinen THE, Franke KJA, van Dijken S (2012) Electric-field control of magnetic domain wall motion and local magnetization reversal. Sci Rep 2:258

185. Geprägs S, Mannix D, Opel M, Goennenwein STB, Gross R (2013) Converse magnetoelectric effects in $Fe_3O_4/BaTiO_3$ multiferroic hybrids. Phys Rev B 88:054412
186. Brintlinger T, Lim S-H, Baloch KH, Alexander P, Qi Y, Barry J, Melngailis J, Salamanca-Riba L, Takeuchi I, Cumings J (2010) In situ observation of reversible nanomagnetic switching induced by electric fields. Nano Lett 10:1219
187. Cherifi RO, Ivanovskaya V, Phillips LC, Zobelli A, Infante IC, Jacquet E, Garcia V, Fusil S, Briddon PR, Guiblin N et al (2014) Electric-field control of magnetic order above room temperature. Nat Mater 13:345
188. Zhang S, Zhao YG, Li PS, Yang JJ, Rizwan S, Zhang JX, Seidel J, Qu TL, Yang YJ, Luo ZL, He Q, Zou T, Chen QP, Wang JW, Yang LF, Sun Y, Wu YZ, Xiao X, Jin XF, Huang J, Gao C, Han XF, Ramesh R (2012) Electric-field control of nonvolatile magnetization in $Co_{40}Fe_{40}B_{20}/Pb(Mg_{1/3}Nb_{2/3})_{0.7}Ti_{0.3}O_3$ structure at room temperature. Phys Rev Lett 108:137203
189. Liu M, Hoffman J, Wang J, Zhang J, Nelson-Cheeseman B, Bhattacharya A (2013) Magnetoelectric coupling effects in multiferroic complex oxide composite structures. Sci Rep 3:1876
190. Wang Z, Zhang Y, Viswan R, Li Y, Luo H, Li J, Viehland D (2014) Electrical and thermal control of magnetic coercive field in ferromagnetic/ferroelectric heterostructures. Phys Rev B 89:035118
191. Wang Z, Zhang Y, Wang Y, Li Y, Luo H, Li J, Viehland D (2014) Magnetoelectric assisted 180° magnetization switching for electric field addressable writing in magnetoresistive random-access memory. ACS Nano 8:7793
192. You L, Wang B, Zou X, Lim ZS, Zhou Y, Ding H, Chen L, Wang J (2013) Origin of the uniaxial magnetic anisotropy in $La_{0.7}Sr_{0.3}MnO_3$ on stripe-domain $BiFeO_3$. Phys Rev B 88:184426
193. Unguris J, Bowden SR, Pierce DT, Trassin M, Ramesh R, Cheong S-W, Fackler S, Takeuchi I (2014) Simultaneous imaging of the ferromagnetic and ferroelectric structure in multiferroic heterostructures. APL Mater 2:076109
194. Lahtinen THE, Shirahata Y, Yao L, Franke KJA, Venkataiah G, Taniyama T, van Dijken S (2012) Alternating domains with uniaxial and biaxial magnetic anisotropy in epitaxial Fe films on $BaTiO_3$. Appl Phys Lett 101:262405
195. Chopdekar RV, Malik VK, Fraile Rodríguez A, Le Guyader L, Takamura Y, Scholl A, Stender D, Schneider CW, Bernhard C, Nolting F, Heyderman LJ (2012) Spatially resolved strain-imprinted magnetic states in an artificial multiferroic. Phys Rev B 86:014408
196. Streubel R, Köhler D, Schäfer R, Eng LM (2013) Strain-mediated elastic coupling in magnetoelectric nickel/barium-titanate heterostructures. Phys Rev B 87:054410
197. Chopdekar RV, Heidler J, Piamonteze C, Takamura Y, Scholl A, Rusponi S, Brune H, Heyderman LJ, Nolting F (2013) Strain-dependent magnetic configurations in manganite-titanate heterostructures probed with soft X-ray techniques. Eur Phys J B 86:241
198. Brandl F, Franke KJA, Lahtinen THE, van Dijken S, Grundler D (2014) Spin waves in CoFeB on ferroelectric domains combining spin mechanics and magnonics. Solid State Commun 198:13
199. Fackler SW, Donahue MJ, Gao T, Nero PNA, Cheong S-W, Cumings J, Takeuchi I (2014) Local control of magnetic anisotropy in transcritical permalloy thin films using ferroelectric $BaTiO_3$ domains. Appl Phys Lett 105:212905
200. Franke KJA, Lahtinen THE, van Dijken S (2012) Field tuning of ferromagnetic domain walls on elastically coupled ferroelectric domain boundaries. Phys Rev B 85:094423
201. Franke KJA, López González D, Hämäläinen SJ, van Dijken S (2014) Size dependence of domain pattern transfer in multiferroic heterostructures. Phys Rev Lett 112:017201
202. O'Handley RC (2000) Modern magnetic materials: principles and applications. Wiley, New York
203. Hubert A (1979) Charged walls in thin magnetic films. IEEE Trans Magn 15:1251

204. Franke KJA, Van de Wiele B, Shirahata Y, Hämäläinen SJ, Taniyama T, van Dijken S (2015) Reversible electric-field driven magnetic domain-wall motion. Phys Rev X 5:011010
205. Van de Wiele B, Laurson L, Franke KJA, van Dijken S (2014) Electric field driven magnetic domain wall motion in ferromagnetic-ferroelectric heterostructures. Appl Phys Lett 104:012401
206. Tsymbal EY, Kohlstedt H (2006) Tunneling across a ferroelectric. Science 313:181
207. Garcia V, Fusil S, Bouzehouane K, Enouz-Vedrenne S, Mathur ND, Barthélémy A, Bibes M (2009) Giant tunnel electroresistance for non-destructive readout of ferroelectric states. Nature 460:81
208. Maksymovych P, Jesse S, Yu P, Ramesh R, Baddorf AP, Kalinin SV (2009) Polarization control of electron tunneling into ferroelectric surfaces. Science 324:1421
209. Gruverman A, Wu D, Lu H, Wang Y, Jang HW, Folkman CM, Zhuravlev MY, Felker D, Rzchowski M, Eom C-B, Tsymbal EY (2009) Tunneling electroresistance effect in ferroelectric tunnel junctions at the nanoscale. Nano Lett 9:3539
210. Crassous A, Garcia V, Bouzehouane K, Fusil S, Vlooswijk AHG, Rispens G, Noheda B, Bibes M, Barthélémy A (2010) Giant tunnel electroresistance with $PbTiO_3$ ferroelectric tunnel barriers. Appl Phys Lett 96:042901
211. Gao XS, Liu JM, Au K, Dai JY (2012) Nanoscale ferroelectric tunnel junctions based on ultrathin $BaTiO_3$ film and Ag nanoelectrodes. Appl Phys Lett 101:142905
212. Pantel D, Goetze S, Hesse D, Alexe M (2011) Room-temperature ferroelectric resistive switching in ultrathin $Pb(Zr_{0.2}Ti_{0.8})O_3$ films. ACS Nano 5:6032
213. Kim DJ, Lu H, Ryu S, Bark C-W, Eom C-B, Tsymbal EY, Gruverman A (2012) Ferroelectric tunnel memristor. Nano Lett 12:5697
214. Chanthbouala A, Crassous A, Garcia V, Bouzehouane K, Fusil S, Moya X, Allibe J, Dlubak B, Grollier J, Xavier S, Deranlot C, Moshar A, Proksch R, Mathur ND, Bibes M, Barthélémy A (2012) Solid-state memories based on ferroelectric tunnel junctions. Nat Nanotechnol 7:101
215. Chanthbouala A, Garcia V, Cherifi RO, Bouzehouane K, Fusil S, Moya X, Xavier S, Yamada H, Deranlot C, Mathur ND, Bibes M, Barthélémy A, Grollier J (2012) A ferroelectric memristor. Nat Mater 11:860
216. Pantel D, Lu H, Goetze S, Werner P, Jik Kim D, Gruverman A, Hesse D, Alexe M (2012) Tunnel electroresistance in junctions with ultrathin ferroelectric $Pb(Zr_{0.2}Ti_{0.8})O_3$ barriers. Appl Phys Lett 100:232902
217. Kim DJ, Lu H, Ryu S, Lee S, Bark CW, Eom CB, Gruverman A (2013) Retention of resistance states in ferroelectric tunnel memristors. Appl Phys Lett 103:142908
218. Soni R, Petraru A, Meuffels P, Vavra O, Ziegler M, Kim SK, Jeong DS, Pertsev NA, Kohlstedt H (2014) Giant electrode effect on tunnelling electroresistance in ferroelectric tunnel junctions. Nat Commun 5:5414
219. Garcia V, Bibes M (2014) Ferroelectric tunnel junctions for information storage and processing. Nat Commun 5:4289
220. Béa H, Bibes M, Cherifi S, Nolting F, Warot-Fonrose B, Fusil S, Herranz G, Deranlot C, Jacquet E, Bouzehouane K, Barthélémy A (2006) Tunnel magnetoresistance and robust room temperature exchange bias with multiferroic $BiFeO_3$ epitaxial thin films. Appl Phys Lett 89:242114
221. Hambe M, Petraru A, Pertsev NA, Munroe P, Nagarajan V, Kohlstedt H (2010) Crossing an interface: ferroelectric control of tunnel currents in magnetic complex oxide heterostructures. Adv Funct Mater 20:2436
222. Yamada H, Garcia V, Fusil S, Boyn S, Marinova M, Gloter A, Xavier S, Grollier J, Jacquet E, Carrtro C, Deranlot C, Bibes M, Barthélémy A (2013) Giant electroresistance of supertetragonal $BiFeO_3$-based ferroelectric tunnel junctions. ACS Nano 7:5385
223. Liu YK, Yin YW, Dong SN, Yang SW, Jiang T, Li XG (2014) Coexistence of four resistance states and exchange bias in $La_{0.6}Sr_{0.4}MnO_3/BiFeO_3/La_{0.6}Sr_{0.4}MnO_3$ multiferroic tunnel junction. Appl Phys Lett 104:043507

224. Boyn S, Girod S, Garcia V, Fusil S, Xavier S, Deranlot C, Yamada H, Carrétéro C, Jacquet E, Bibes M, Barthélémy A, Grollier J (2014) High-performance ferroelectric memory based on fully patterned tunnel junctions. Appl Phys Lett 104:052909
225. Zhuravlev MY, Sabirianov RF, Jaswal SS, Tsymbal EY (2005) Giant electroresistance in ferroelectric tunnel junctions. Phys Rev Lett 94:246802
226. Kohlstedt H, Pertsev NA, Rodríguez Contreras J, Waser R (2005) Theoretical current–voltage characteristics of ferroelectric tunnel junctions. Phys Rev B 72:125341
227. Ikeda S, Hayakawa J, Ashizawa Y, Lee YM, Miura K, Hasegawa H, Tsunoda M, Matsukura F, Ohno H (2008) Tunnel magnetoresistance of 604% at 300 K by suppression of Ta diffusion in CoFeB/MgO/CoFeB pseudo-spin-valves annealed at high temperature. Appl Phys Lett 93:082508
228. Valencia S, Crassous A, Bocher L, Garcia V, Moya X, Cherifi RO, Deranlot C, Bouzehouane K, Fusil S, Zobelli A, Gloter A, Mathur ND, Gaupp A, Abrudan R, Radu F, Barthélémy A, Bibes M (2011) Interface-induced room-temperature multiferroicity in $BaTiO_3$. Nat Mater 10:753
229. Wen Z, Li C, Wu D, Li A, Ming N (2013) Ferroelectric-field-effect-enhanced electroresistance in metal/ferroelectric/semiconductor tunnel junctions. Nat Mater 12:617